



PATENT  
Attorney Docket No.: 019633-000810US  
Client Ref. No.: NRC00027US; NRC IPSO 10875

**IN THE UNITED STATES PATENT AND TRADEMARK OFFICE**

In re application of:

MICHEL GILBERT et al.

Application No.: 09/211,691

Filed: December 14, 1998

For: FUSION PROTEINS FOR USE IN  
ENZYMATIC SYNTHESIS OF  
OLIGOSACCHARIDES

Customer No.: 20350

Confirmation No. 9572

Examiner: Rao, Manjunath

Technology Center/Art Unit: 1652

DECLARATION OF DR. JAMES  
PAULSON UNDER 37 C.F.R. §1.132

Commissioner for Patents  
P.O. Box 1450  
Alexandria, VA 22313-1450

Sir:

I, James C. Paulson, Ph.D., being duly warned that willful false statements and the like are punishable by fine or imprisonment or both (18 U.S.C. § 1001), and may jeopardize the validity of the patent application or any patent issuing thereon, state and declare as follows:

1. All statements herein made of my own knowledge are true, and statements made on information or belief are believed to be true and correct.

2. I am currently a Professor in the Department of Molecular Biology at the Scripps Research Institute in La Jolla, California. I am a Principle Investigator for the Consortium of Functional Glycomics, a multi-institution, multi-disciplinary research initiative funded by the National Institute of General Medical Sciences to understand the role of carbohydrate-protein interactions at the cell surface in cell-cell communication. I am also co-chair of the Human Glycomics/Proteomics Initiative, another multi-institution, multi-disciplinary

**EXHIBIT A**

research initiative to identify glyco-biomarkers for diagnosis, monitoring, and treatment of human disease.

3. I received an A.B. in chemistry and biology in 1970 from MacMurray College. I received an M.S. in Biochemistry in 1971 and a Ph.D. in Biochemistry in 1974, both from the University of Illinois at Champaign-Urbana. I was a postdoctoral fellow in the Department of Biochemistry at Duke University Medical Center in Durham, N.C. from 1974-1978. From 1978 to 1990 I was a faculty member in the Department of Biological Chemistry at the UCLA School of Medicine in Los Angeles, California with the following appointments: Assistant Professor (1978-1981), Associate Professor (1981-1985) and Professor and Vice-Chair (1985-1990). From 1990 to 1999 I was employed at Cytel Corporation in San Diego, California first as Vice President of Research and Development (1990-1996) and then Vice President, Chief Scientific Officer and General Manager of Glytec, a division of Cytel (1996-1999). Since 1999 I have been a Professor in the Department of Molecular Biology at the Scripps Research Institute in La Jolla, California. I am a member the American Chemical Society, the American Society of Biological Chemists, and the Society for Complex Carbohydrates. I served as President of the Society for Glycobiology in 2002 and 2003. Since 1990 I have been on the editorial board of *Glycobiology*. From 1985 through 1991 I was on the editorial board of *Journal of Biological Chemistry*. I am an author on 204 peer-reviewed journal articles. I have also authored or co-authored 21 book chapters. A copy of my curriculum vitae is attached hereto as Exhibit B.

3. The present invention is nucleic acids that encode fusion proteins comprising an  $\alpha$ -2,3-sialyltransferase that catalyzes the transfer of a sialic acid, from CMP-Neu5Ac, to an acceptor molecule; and a CMP-Neu5Ac synthetase that catalyzes the formation of CMP-Neu5Ac from Neu5Ac and CTP.

4. I have read and am familiar with the contents of this patent application. In addition, I have read an Office Action, dated May 6, 2005, received in the present case. It is my

understanding that the Examiner alleges that the claimed invention is obvious in view of Bulow *et al.*, *TIBtech* 9:226-231 (1991); Defrees *et al.*, WO 96/32491; and the common knowledge of the art of molecular biology provided by Sambrook *et al.*, pages 7.37-7.52 (1989) in further view of Gilbert(a) *et al.* *Eur. J. Biochem.*, 249:187-194 (1997) and Gilbert(b) *et al.* *Biotech. Lett.* 19:417-420 (1997). In addition, the Examiner cites Warner, *Nat. Biotech.* 16:720-721 (1998).

5. The Examiner appears to rely most heavily on the disclosure of Bulow *et al.* as providing a motivation to construct a bi-functional protein after fusing mono-functional proteins together. According to the Examiner, Bulow *et al.* teaches that construction of fusion proteins results in favorable enzyme kinetics. Office Action at page 3. The Examiner also asserts at page 7 of the Office Action that the improved properties of the claimed fusion protein depend on the "proximity effect" as taught by Bulow *et al.*

6. Bulow *et al.* was published in 1991. When the application was in filed 1997, questions had been raised about the validity of proximity effect disclosed in Bulow *et al.* The simplest model of a proximity effect relies on diffusion or Brownian motion for transport of a reaction intermediate between two active sites on a bi-functional fusion protein. However, researchers demonstrated that Brownian motion was not sufficient to transfer a coupled reaction intermediate from the active site of one protein to the active site of its fusion partner. *See, e.g.*, Elcock and McCammon, *Biochemistry* 35:12652-12658 (1996), page 12652, right column; submitted as Exhibit C. Researchers then proposed that the arrangement of charged residues on a fusion protein allowed electrostatic surface diffusion or channeled transfer of an intermediate from the active site of one protein to the active site of its fusion partner. Again, this channeled transfer or substrate channeling was believed to enhance reaction kinetics and explain the so-called proximity effect.

7. Researchers were not able to reproduce substrate channeling in a synthetic bi-functional fusion protein, even though the structure of a naturally occurring bi-functional

fusion protein, the *Leishmania* dihydrofolate reductase-thymidylate synthase (DHFR-TS) was available as a model. *E. coli* express DHFR and TS as two separate mono-functional enzymes. Researchers fused the *E. coli* enzymes to make a synthetic bi-functional DHFR-TS fusion protein modeled after the *Leishmania* DHFR-TS. See, e.g., Trujillo *et al.*, *Prot. Eng.* 10:567-573 (1997), submitted as Exhibit D. However, the synthetic *E. coli* DHFR-TS bi-functional fusion protein did not exhibit substrate channeling. Trujillo *et al.* concluded that "the local concentration of H<sub>2</sub>-folate obtained by linking the mono-functional *E. coli* enzymes is not sufficient to promote substrate channeling." See, e.g., Trujillo *et al.* at page 572, right column. Thus, Trujillo *et al.* demonstrated that substrate channeling, *i.e.*, a proximity effect, did not occur in the synthetic *E. coli* DHFR-TS fusion protein.

8. The May 1997 Trujillo *et al.* article raises doubts about the validity of the proximity effect in at least two ways. First, even though the authors of Trujillo *et al.* used the naturally-occurring *Leishmania* DHFR-TS bi-functional fusion protein as a structural model, they could not reconstitute a proximity effect in the synthetic *E. coli* DHFR-TS bi-functional fusion protein. Second, researchers who studied the family of DHFR and TS proteins had postulated that the naturally occurring bi-functional DHFR-TS proteins have a functional advantage over the naturally occurring non-fused enzymes, *i.e.*, enhanced enzyme kinetics resulting from substrate channeling. However, the occurrence of unfused enzymes in some species, *i.e.*, *E. coli*, indicates that any "advantage" resulting from alleged proximity effects is not conserved during evolution. Therefore, in May 1997 the proximity effect could not reliably be generated in synthetic fusion proteins, and the proposed advantage of a bi-functional fusion protein over mono-functional proteins was doubted.

9. Finally, papers that build on the results of Trujillo *et al.* and discredit the proximity effect continue to be published. One particularly interesting paper, Pettersson *et al.* *Eur. J. Biochem.* 267:5041-5046 (2000), demonstrates that a model for proximity effect based on fusion of malate dehydrogenase and citrate synthase is incorrect. Lief Bulow, the author of the

PATENT

Atty. Docket No. 019633-000810US

Appln. No. 09/211,691


Bulow reference cited in the Office Action, is also an author of Pettersson *et al.*, and thus, appears to be in agreement that the proximity effect is not valid. Pettersson *et al.* state at 5045, right column . . . "[B]ringing two sequential enzymes together in a fusion protein . . . is obviously not sufficient to cause any kinetically significant metabolite channeling through proximity effects." Pettersson *et al.* is submitted as Exhibit E.

10. The proximity effect disclosed in Bulow *et al.* was not established at the time of filing and continues to be discredited. Bulow *et al.* provide only a few examples of bi-functional fusion proteins, and do not disclose a fusion of a glycosyltransferase and an accessory enzyme. Bulow *et al.* did not provide disclosure to suggest that fusion a glycosyltransferase and an accessory enzyme could be fused to make an active bi-functional fusion protein. Therefore, one of skill would not have been motivated to fuse a glycosyltransferase and an accessory enzyme based on the disclosure of Bulow *et al.*

Date:

March 8, 2006

By:

  
James C. Paulson, Ph.D.

60680012 v1

## CURRICULUM VITAE

**James C. Paulson**

Professor  
Department of Molecular Biology  
Department of Molecular Experimental Medicine  
10550 North Torrey Pines Road, MEM-L71  
La Jolla, CA 92037  
858-784-9634 (Phone)  
858-784-9690 (Fax)  
[jpaulson@scripps.edu](mailto:jpaulson@scripps.edu)  
<http://www.scripps.edu/mb/paulson/>



Spouse: Beverly Moore Paulson  
Children: Lorien Mary, Erik Richard, Evan Carsten

### PROFESSIONAL POSITIONS:

1999-present Professor, Department of Molecular Biology & Department of Molecular Experimental Medicines, The Scripps Research Institute, La Jolla, CA  
1996-1999 Vice President, Chief Scientific Officer, General Manager Glytec Division, and Member Board of Directors, Cytel Corporation, San Diego, CA  
1990-1996 Vice Pres. Res. Dev. and Member of Board of Directors, Cytel Corp., San Diego, CA  
1985-1990 Professor and Vice-Chair, Dept. of Biol.Chem., UCLA Sch. of Medicine, Los Angeles, CA  
1981-1985 Associate Professor, Dept of Biol. Chem., UCLA School of Medicine, Los Angeles, CA  
1978-1981 Assistant. Professor, Dept. of Biol. Chem., UCLA School of Medicine, Los Angeles, CA  
1974-1978 Postdoctoral Fellow/Res. Assoc., Dept. of Biochem., Duke Univ. Med. Ctr, Durham, NC

### EDUCATION:

University of Illinois at Champaign-Urbana  
Ph.D. (Biochemistry) 1974  
M.S. (Biochemistry) 1971  
MacMurray College, Jacksonville, Illinois  
A.B.(Chemistry/Biology)1970

### PROFESSIONAL ACTIVITIES:

2001-present Principle Investigator, Consortium Functional Glycomics, <http://www.functionalglycomics.org>  
2005-present Co-chair Human Glycomics/Proteomics Initiative (HGPI), <http://www.hgpi.jp>  
2002-2003 President, The Society for Glycobiology  
2004-present Scientific Advisor, Nexbio  
1999-present Scientific Advisory Board, Neose Technologies Inc  
1996-present Honorary Member, American Society of Clinical Investigation  
1990-present Editorial Board, Glycobiology  
1990-present Member, American Chemical Society  
1989-1999 Scientific Advisory Board, Complex Carbohydrate Resource Center, Univ. Georgia  
1989-1991 NIH Study Section, Pathobiochemistry  
1986-1988 Scientific Advisory Board, Nucleic Acid Research Institute  
1985-1991 Editorial Board, Journal of Biological Chemistry  
1980-present Member, American Society of Biological Chemists  
1979-present Member, Society for Complex Carbohydrates

## **PATENTS AND PATENT APPLICATIONS:**

Antigenic compositions and methods for using the same

Reiko F. Irie, Tadashi Tai, Donald L. Morton, Leslie D. Cahan, James C. Paulson

Patent issued December 10, 1985. #4,557,931

Method for producing secretable glycosyltransferases and other processing enzymes

James C. Paulson, Eryn Ujita-Lee, Beverly Adler, Jeffrey K. Browne, Jasminder Weinstein

Patents issued: #5,032,519, #5,541,083; #5,776,772

Process for controlling intracellular glycosylation of proteins.

James Paulson, Eryn Ujita-Lee, Jasminder Weinstein

Patent issued September 10, 1991 #5,047,335

Intercellular adhesion mediators

James Paulson, Mary Perez, Federico Gaeta, and Murray Ratcliffe

Patent issued May 19, 1998 #5,753,631

Compositions and methods for the identification and synthesis of sialyltransferases

James Paulson, Dawn Wen, Brian Livingston, Bill Giles, Sørge Kelm, Kati Medzerhadsky, Alan Burlingham

Patent issued January 12, 1999 #5,858,751; October 5, 1999 #5,962,294

Antibodies to P-selectin and their uses

Robert Chestnut, Margaret Polley and James Paulson

Patent issued September 1, 1998 #5,800,815

Use of trans-sialidase and sialyltransferase for synthesis of sialyl-2-3-betagalactosides

Yukishige Ito and James Paulson

Patent issued April 4, 1995, #5,409,817

Practical In vitro sialylation of recombinant glycoproteins

James C. Paulson, Eric Sjøberg and Bob Bayer

Patent issued June 4, 2002, #6,399,336

Control of Immune Responses by Modulating Sialyltransferases

Jamey Marth and James Paulson

Patent issued June 4, 2002, #6,376,475

Method for Detecting the Presence of P-Selectin

Robert Chestnut, Margaret Polley and James Paulson

Patent issued March 7, 2000, #6,033,667

Practical in vitro Sialylation of Recombinant Glycoproteins

James Paulson, Robert Bayer, and Eric Sjøberg

Patent issued June 4, 2002, #6,399,336B1

## RECENT PUBLICATIONS (from a total of >200):

1. Collins, B.E., Smith, B.A., Bengtson, P., and Paulson, J.C. (2006) Ablation of CD22 in ligand-deficient mice restores B cell receptor signaling. *Nature Immunol.* 7:199-206
2. Han, S., Collins, B.E., and Paulson, J.C. (2006) Synthesis of 9-Substituted Sialic Acids As Probes for CD22-Ligand Interactions on B., ACS Symp. Ser., in press.
3. Comelli, E.M., Head, S.R., Gilmartin, T., Whisenant, T., Haslam, S.M., North, S.J., Wong, N.K., Kudo, T., Narimatsu, H., Esko, J.D., Drickamer, K., Dell, A., and Paulson, J.C. (2006) A Focused Microarray Approach to Functional Glycomics: Transcriptional Regulation of the Glycome. *Glycobiology.* 16:117-131
4. Stevens, J., Blixt, O., Glaser, L., Taubenberger, J.K., Palese, P., Paulson, J.C., and Wilson, I.A. (2006) Glycan Microarray Analysis of the Hemagglutinins from Modern and Pandemic Influenza Viruses Reveals Different Receptor Specificities. *J. Mol. Biol.* 355:1143-55
5. Taniguchi, N., Nakamura, K., Narimatsu, H., von der Lieth, C.W., and Paulson, J.C. (2006) Human Disease Glycomics/Proteome Initiative Workshop and the 4th HUPO Annual Congress. *Proteomics.* 6:12-3.
6. Raman, R., Raguram, S., Venkataraman, G., Paulson, J.C., and Sasisekharan, R. (2005) Glycomics: an integrated systems approach to structure-function relationships of glycans. *Nature Methods* 2:817-824.
7. Tateno, H., Crocker, P. and Paulson, J.C. (2005) Mouse Siglec-F and Human Siglec-8 are functionally convergent paralogs that are selectively expressed on eosinophils and recognize 6'-Sulfo-Sialyl Lewis X as a preferred glycan ligand. *Glycobiology.* 15:1125-1135
8. Han, S., Collins, B.E., Bengtson, P. and Paulson, J.C. (2005) Homo-multimeric Complexes of CD22 in B cells Revealed by Protein-Glycan Crosslinking. *Nature Chem. Biol.* 1:93-97
9. Blixt, O., Vasiliu, D., Allin, K., Jacobsen, N., Warnock, D., Razi, N., Paulson, J.C., Bernatchez, S., Gilbert, M., and Wakarchuk, W. (2005) Chemoenzymatic Synthesis of 2-azidothyl-Ganglio-oligosaccharides GD3, GT3, GM2, GD2, GT2, GM1, and GD1a. *Carbohydrate Research.* 340:1963-72
10. Vyas, A.A., Blixt, O., Paulson, J.C., and Schnaar, R.L. (2005) Potent Glycan Inhibitors of Myelin-associated Glycoprotein Enhance Axon Outgrowth in Vitro. *J. Biol. Chem.* 280:16305-10
11. Goldberg, D., Sutton-Smith, M., Paulson, J.C., and Dell, A. (2005) Automatic annotation of matrix-assisted laser desorption/ionization N-glycan spectra. *Proteomics.* 5:865-875
12. Kitazume, S., Nakagawa, K., Oka, R., Tachida, Y., Ogawa, K., Luo, Y., Citron, M., Shitara, H., Taya, C., Yonekawa, H., Paulson, J.C., Miyoshi, E., Taniguchi, N., and Hashimoto, Y. (2005) In vivo cleavage of alpha 2,6-sialyltransferase by Alzheimer's beta -secretase. *J. Biol. Chem.* 280:8589-8595
13. Blixt, O., Head, S., Mondala, T., Scanlan, C., Huflejt, M.E., Alvarez, R., Bryan, M.C., Fazio, F., Calarese, D., Stevens, J., Razi, N., Stevens, D.J., Skehel, J.J., van Die, I., Burton, D.R., Wilson, I.A., Cummings, R., Bovin, N., Wong, C-H., and Paulson, J.C. (2004) Printed Covalent Glycan Array for Ligand Profiling of Diverse Glycan Binding Proteins. *Proc. Natl. Acad. Sci. USA* 101:17033-17038
14. Collins, B.E. and Paulson, J.C. (2004) Cell Surface Biology Mediated by Low Affinity Multivalent Protein-Glycan Interactions. *Curr. Opin. Chem. Biol.* 8:617-625.
15. Ikehara, Y., Ikehara, S.K., and Paulson, J.C. (2004) Negative regulation of T cell receptor signaling by Siglec-7 (p70/AIRM) and Siglec-9. *J. Biol. Chem.* 279:43117-43125
16. Amado, M., Qi, Y., Comelli, E.M., Collins, B. and Paulson, J.C. (2004) PNA high phenotype of activated CD8+ T cells results from de novo synthesis of CD45 glycans. *J. Biol. Chem.* 279(35):36689-97.
17. Collins, B. E., Blixt, O., DeSieno, A. R., Bovin, N., Marth, J. D. & Paulson, J.C. (2004) Masking of CD22 by cis ligands does not prevent redistribution of CD22 to sites of cell contact. *Proc. Natl. Acad. Sci. USA* 101:6104-6109.
18. Bryan, M.C., Fazio, F., Lee, H-K., Huang, C-Y., Chang, A., Best, M.D., Calarese, D.A., Blixt, O., Paulson, J.C., Burton, D., Wilson, I.A., & Wong, C-H. (2004) Covalent display of oligosaccharide arrays in microtiter plates. *J. Amer. Chem. Soc.* 126:8640-8641.
19. Shen, A., Go, E.P., Gamez, A., Apon, J.V., Fokin, V., Greig, M., Ventura, M., Crowell, J.E., Blixt, O.,



- Paulson, J.C., Stevens, R.C., Finn, M.G. & Siuzdak, G. (2004) A Mass Spectrometry Plate Reader: Monitoring Enzyme Activity and Inhibition with a Desorption/Ionization on Silicon (DIOS) Platform. *Chem. Bio. Chem.* 5:921-927
20. Blixt, O., Collins, B.E., Van Den Nieuwenhof, I.M., Crocker, P.R., and Paulson, J.C. (2003) Sialoside Specificity of the Siglec Family Assessed Using Novel Multivalent Probes: IDENTIFICATION OF POTENT INHIBITORS OF MYELIN-ASSOCIATED GLYCOPROTEIN. *J. Biol. Chem.* 278:31007-19.
  21. Comelli, E. M., Amado, M., Lustig, S. R., and Paulson, J. C. (2003) Identification and expression of Neu4, a novel murine sialidase. *Gene* 321:155-161.
  22. Blixt, O. and Paulson, J.C. (2003) Biocatalytic Preparation of N-Glycolylneuraminic Acid, Deaminoneuraminic Acid (KDN) and 9-Azido-9-deoxysialic Acid Oligosaccharides. *Adv. Synth. Catal.* 345:687-690.
  23. Kalovidouris, S.A., Blixt, O., Nelson, A., Vidal, S., Turnbull, W.B, Paulson, J.C., and Stoddart, J.F. (2003) Chemically Defined Sialoside Scaffolds for Investigations with Sialic Acid Binding Proteins. *J. Org. Chem.* 68:8485-8493.
  24. Danzer, C.P., Collins, B.E., Blixt, O., Paulson, J.C., and Nitschke, L. (2003) Transitional and marginal zone B cells have a high proportion of unmasked CD22: implications for BCR signaling. *Int. Immunol.* 15:1137-1147.
  25. Zuber, C., Paulson, J.C., Toma, V., Winter, H.C., Goldstein, I.J., and Roth, J. (2003) Spatiotemporal expression patterns of sialoglycoconjugates during nephron morphogenesis and their regional and cell type-specific distribution in adult rat kidney. *Histochem. Cell Biol.* 120:143-60.
  26. Comelli, E., Amado, M., Head, S., and Paulson, J.C. (2002) Custom microarray for glycobologists: considerations for glycosyltransferases gene expression profilin. K. Drickamer and A. Dell (eds.), In *Glycogenomics: the Impact of Genomics and Informatics on Glycobiology*, vol. 69. Portland Press Ltd, London, p. 135-42.
  27. Collins, B.E., Blixt, O., Bovin, N. V., Danzer, C.P., Chui, D., Marth, J.D., Nitschke, L., and Paulson, J.C. (2002) Constitutively unmasked CD22 on B cells of ST6Gal I knockout mice: novel sialoside probe for murine CD22. *Glycobiology* 12:563-71.
  28. Blixt, O., Allin, K., Pereira, L., Datta, A., and Paulson, J.C. (2002) Efficient chemoenzymatic synthesis of o-linked sialyl oligosaccharides. *J. Amer. Chem. Soc.* 124:5739-46.
  29. Fazio, F., Bryan, M.C., Blixt, O., Paulson, J.C., and Wong, C.H. (2002) Synthesis of Sugar Arrays in Microtiter Plate. *J. Amer. Chem. Soc.* 124:14397-14402.
  30. Dormitzer, P.R., Sun, Z. Y., Blixt, O., Paulson, J. C., Wagner, G., and Harrison, S.C. (2002) Specificity and Affinity of Sialic Acid Binding by the Rhesus Rotavirus VP8\* Core. *J. Virol.* 76:10512-10517.
  31. Saito, S., Yamashita, S., Endoh, M., Yamato, T., Hoshi, S., Ohyama, C., Watanabe, R., Ito, A., Satoh, M., Wada, T., Paulson, J.C., Arai, Y., and Miyagi, T. (2002) Clinical significance of ST3Gal IV expression in human renal cell carcinoma. *Oncol. Rep.* 9:1251-5.
  32. Lee, K. J., Mao, S., Sun, C., Gao, C., Blixt, O., Arrues, S., Hom, L.G., Kaufmann, G.F., Hoffman, T.Z., Coyle, A.R., Paulson, J.C., Felding-Habermann, B., and Janda, K. D. (2002) Phage-display selection of a human single-chain fv antibody highly specific for melanoma and breast cancer cells using a chemoenzymatically synthesized G(M3)-carbohydrate antigen. *J. Amer. Chem. Soc.* 124:12439-46.

**For additional listing from 2001 to 1973 see <http://www.scripps.edu/mb/paulson/publications.html>**

*Accelerated Publications*

## Evidence for Electrostatic Channeling in a Fusion Protein of Malate Dehydrogenase and Citrate Synthase<sup>†</sup>

Adrian H. Elcock\* and J. Andrew McCammon

*Department of Chemistry and Biochemistry and Department of Pharmacology, University of California at San Diego, La Jolla, California 92093-0365**Received June 20, 1996; Revised Manuscript Received August 2, 1996<sup>®</sup>*

**ABSTRACT:** Brownian dynamics simulations were performed to investigate a possible role for electrostatic channeling in transferring substrate between two of the enzymes of the citric acid cycle. The diffusion of oxaloacetate from one of the active sites of malate dehydrogenase (MDH) to the active sites of citrate synthase (CS) was simulated in the presence and absence of electrostatic forces using a modeled structure for a MDH–CS fusion protein. In the absence of electrostatic forces, fewer than 1% of substrate molecules leaving the MDH active site are transferred to CS. When electrostatic forces are present at zero ionic strength however, around 45% of substrate molecules are successfully channeled. As expected for an electrostatic mechanism of transfer, increasing the ionic strength in the simulations reduces the calculated transfer efficiency. Even at 150 mM however, the inclusion of electrostatic forces results in an increase in transfer efficiency of more than 1 order of magnitude. The simulations therefore provide evidence for the involvement of electrostatic channeling in guiding substrate transfer between two of the enzymes of the citric acid cycle. Similar effects may operate between other members of the citric acid metabolon.

The association of enzymes involved in a particular metabolic pathway into a single multienzyme complex is a well-known phenomenon, with perhaps the most prominent example being the pyruvate dehydrogenase complex (Reed, 1974) responsible for production of acetyl coenzyme A. The purported advantages of forming such multienzyme complexes seem intuitively reasonable (Welch, 1977; Sreere, 1985): the close proximity of enzymes responsible for catalyzing consecutive steps of a metabolic cycle may reduce the time required for substrate to diffuse between enzymes and prevent the substrate from escaping into solution where it might be sequestered by other enzymes for use in different metabolic pathways. This latter aspect may be particularly important for maintaining metabolic flux with low overall concentrations of metabolite (Welch, 1977).

In principle, consecutive enzymes in a multienzyme complex might be close enough together that simple random diffusion would be sufficient to provide an efficient means of transferring substrate between active sites. Recent experimental and theoretical work suggests however that the efficiency of substrate transfer might be dramatically enhanced by electrostatic effects. This idea stems largely from the solution of the crystal structure of the protozoan bifunctional enzyme dihydrofolate reductase–thymidylate synthase (DHFR–TS)<sup>†</sup> (Knighton *et al.*, 1994). DHFR and TS catalyze sequential steps in the thymidylate cycle, with

the dihydrofolate (FH<sub>2</sub>) produced by the TS-catalyzed reaction subsequently acting as the substrate for the DHFR-catalyzed reaction. Experimentally the bifunctional form of the enzyme has been shown to have significant kinetic advantages over the related monofunctional enzymes in terms of a markedly reduced lag time for appearance of the final products of the coupled system (Meek *et al.*, 1984). The crystal structure of DHFR–TS shows the entrances to the active sites to be at the enzyme surface and separated by around 40 Å. Lying between the two active sites is a number of positively charged residues which were hypothesized to guide FH<sub>2</sub>, which has a net charge of –2e, from the TS to the DHFR active site. Strong support for this idea has come from Brownian dynamics (BD) simulations of the process of substrate transfer (Elcock *et al.*, 1996). In simulations conducted at zero ionic strength the efficiency with which substrate was transferred from the TS to the DHFR active site was found to be almost 100%. Perhaps more importantly, the simulations suggested that uncharged substrates, which experience no electrostatic guidance mechanism, are transferred with an efficiency of only around 5%: much too low to explain the experimental observation of efficient channeling. Further support for electrostatic channeling in DHFR–TS has been provided by recent experimental work showing that the efficiency of substrate transfer is dependent on ionic strength (Trujillo *et al.*, 1995, 1996); this result,

<sup>†</sup> This work was supported by the Wellcome Trust under Grant 041157/Z/94/Z and by grants from the National Institutes of Health, the National Science Foundation, and the National Science Foundation MetaCenter Program.

<sup>®</sup> Abstract published in *Advance ACS Abstracts*, September 1, 1996.

<sup>1</sup> Abbreviations: CS, citrate synthase; MDH, malate dehydrogenase; PB, Poisson–Boltzmann; BD, Brownian dynamics; DHFR–TS, dihydrofolate reductase–thymidylate synthase; NADH, nicotinamide adenine dinucleotide (reduced); AAT, aspartate aminotransferase.

which was also reflected in the simulations, is an expected characteristic of an electrostatic mechanism of transfer.

Given the apparent importance of electrostatic effects suggested by both experimental and theoretical results for DHFR-TS, it is clearly of considerable interest to ask whether a similar mechanism operates elsewhere in nature. The focus of the present work is therefore on investigating the possible role of an electrostatic channeling mechanism in transferring substrate oxaloacetate between the citric acid cycle enzymes malate dehydrogenase (MDH) and citrate synthase (CS). Recent experimental work (Lindblah *et al.*, 1994) has described the preparation and characterization of a fusion protein of the yeast forms of the two enzymes in which the C-termini of CS are connected by a short linker sequence (Gly-Ser-Gly) to the N-termini of MDH. Kinetics studies of the fusion protein resulted in two findings that suggest that oxaloacetate is efficiently channeled between MDH and CS. First, the lag (transient) time for formation of the final products (NADH and citrate) in the fusion protein was shorter than in the free enzymes; the lag time was also shorter than the theoretical estimate based on the ratio of  $v_{\max}$  and  $K_m$  for the CS part of the coupled system (Easterby, 1973). Second, addition of aspartate aminotransferase (AAT), which competes with CS for the intermediate substrate oxaloacetate, had much less of an effect on the steady-state rate of the fusion protein than that of the free enzymes, an observation that indicates that oxaloacetate is largely sequestered from the bulk solution.

From a simulation viewpoint the MDH-CS fusion protein is attractive since good structural information, a prerequisite for theoretical work, is available for each of the individual components of the system. While crystal structures of the yeast forms of the enzymes have not been solved, structures are available for the pig heart forms of both enzymes, and these are expected to be good models for the yeast enzymes. The problem of docking the two enzymes together in some reasonable fashion remains of course, but the use in the experimental work of a very short linker region (three amino acids) to connect the CS and MDH enzymes means that the orientational possibilities for such a fusion protein are drastically reduced. In fact, this sufficiently constrains the system that it is possible for a model of the fusion protein to be constructed by simply docking the CS and MDH structures so that the CS C-termini are adjacent to the MDH N-termini (Lindblah *et al.*, 1994).

A model of the fusion protein built in this way has the MDH and CS active sites separated by nearly 60 Å, with the MDH active site facing away from CS. This is such a large distance that it would appear at first sight unlikely that substrate would be transferred between active sites with any great efficiency: certainly, it appears to have prompted Srere and co-workers to consider the possibility of a dimer of the fusion protein being responsible for efficient channeling (Lindblah *et al.*, 1994). We report here, however, the results of BD simulations which suggest that, even in a monomer of the fusion protein, an electrostatically based channeling mechanism can be surprisingly efficient.

## MATERIALS AND METHODS

All BD simulations were performed with the program UHBD (Madura *et al.*, 1994, 1995). The crystal structures of MDH (Gleason *et al.*, 1994) and CS (Remington *et al.*,

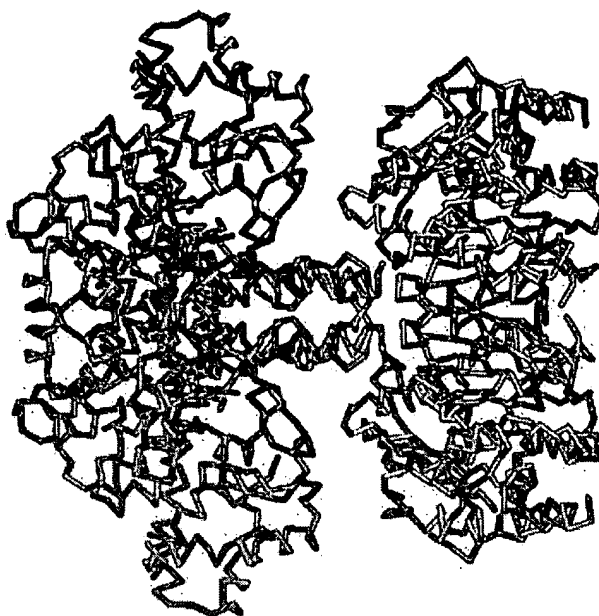


FIGURE 1:  $\alpha$  trace of the MDH-CS fusion protein model. The CS dimer is shown in red, with the three C-terminal residues of each monomer colored purple. The MDH dimer is shown in blue, with the three N-terminal residues of each monomer colored green. This figure was prepared using the program QUANTA.

1982) (both of which are dimers) were used as the starting point for generating a model of the fusion protein. The "open" form of CS was used as it has been suggested to represent a substrate entry/product release form of the enzyme (Remington *et al.*, 1982). Bound citrate molecules were removed from both the MDH and CS structures. Hydrogens were added to each enzyme using the molecular simulation program CHARMM (Brooks *et al.*, 1983). Titratable residues were assumed to be in their usual protonation state at pH 7; i.e., the net charge of all Asp and Glu residues was set to  $-1e$  and all Arg and Lys residues set to  $+1e$ ; protonation states for histidines were assigned on the basis of their local environment, and all were in neutral forms. The total charge on the MDH dimer was therefore  $+6e$ ; that on the CS dimer was  $-2e$ . The two enzymes were docked so that the C-termini of the CS dimer were within 5 Å of the N-termini of the MDH dimer and so that structural overlap was kept to a minimum (Figure 1). A more refined method of docking involving energy minimization of the resulting structure could of course be envisaged, but the structural uncertainties involved are large enough at this stage that we feel that such an approach would not be justified; in any case, the results are not likely to be altered significantly.

Prior to BD simulations being performed, the electrostatic potential around the fusion protein was obtained by finite-difference solution of the linear Poisson-Boltzmann equation (Honig & Nicholls, 1995) using a  $160^3$  grid of spacing 1.2 Å. Boundary potentials were set assuming that each charge in the system is subject to Debye-Hückel screening. Atomic radii and charges were obtained from the CHARMM22 parameter set (Mackerell *et al.*, 1995). The internal dielectric of the protein was set to 4.0 while that of the solvent was set to 78.0, appropriate for water at 25 °C. The ionic strength was set to 0 mM in most simulations, although a range of values between 0 and 150 mM was used to investigate the ionic strength dependence of transfer efficiency. Oxalo-

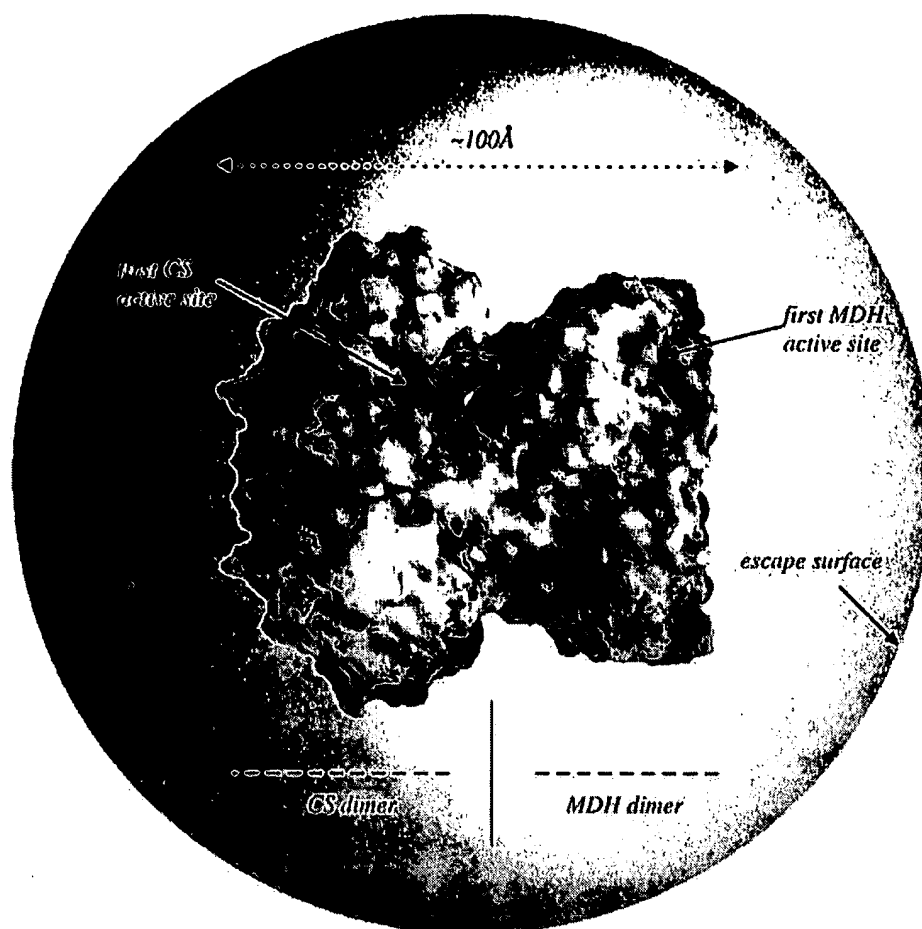


FIGURE 2: MDH-CS system viewed from a similar position to that in Figure 1. The molecular surface of the protein is colored according to the electrostatic potential calculated at zero ionic strength. Blue areas on the molecular surface represent electrostatically positive regions; red, electrostatically negative regions (limits set at  $\pm 15$  kT). The green area indicates the substrate starting point at the first MDH monomer's active site. The purple area marks the substrate reaction region at the first (most favored) CS active site. The second (less favored active site) CS active site is around the back of the figure. Substrate molecules reaching the purple surface are assumed to react at the CS active sites. The large sphere marks a radius 90 Å from the center of the protein: substrate molecules which reach any point on this surface are considered to have escaped to bulk solution. This figure was prepared using the program GRASP.

acetate was modeled as a sphere of radius 2 Å and charge  $-2e$ ; as in previous work (Elcock *et al.*, 1996) this does not represent a particularly realistic description of the substrate's atomic level structure, but electrostatic channeling effects, *if present*, are likely to be largely accounted for by the overall charge of the substrate. Simple spherical models of substrate have worked well in other simulations, for example in studies of the diffusion of acetylcholine to the active site of acetylcholinesterase (Antosiewicz *et al.*, 1995). A series of BD simulations were performed starting from 1180 different positions evenly distributed over a surface 12 Å from the position of the C1 atom of the bound citrate molecule in the active site of the first MDH monomer. These starting points are located adjacent to the flexible loop formed by residues 77–87 known to play a role in substrate binding (Gleason *et al.*, 1994); these points therefore appear to be a reasonable model for the location of oxaloacetate emerging from the MDH active site. Substrate trajectories were simulated using the Ermak–McCammon algorithm (Ermak & McCammon, 1978) with a time step of 0.05 ps. Trajectories were propagated until one of the following criteria were satisfied: (1) the substrate “reacted” at the CS active sites; (2) the substrate reached a distance of 90 Å from the center of the fusion protein (at which point it was assumed to have

escaped to bulk solution (see Figure 2)); (3) the trajectory exceeded  $1 \times 10^6$  steps. The last criterion was required because a few simulations remained trapped at the MDH active site where they would have stayed indefinitely; such trajectories were omitted from the analysis of results. A “reaction” was assumed to occur when the substrate came within 8 Å of the position of the C3 atom of the bound citrate molecule observed at the active sites of the CS crystal structure (Remington *et al.*, 1982). An 8 Å distance was selected since it gives a reaction region small enough that it provides a good definition of the active site area but sufficiently large that it is unaffected by changing the molecule's grid positioning; the results reported here are not sensitive to this choice of reaction distance. Substrate transfer efficiency was calculated as the percentage of trajectories which terminate successfully at one or other of the CS active sites.

## RESULTS

In the simulations, the efficiency of substrate transfer from the MDH active site to either of the CS active sites is strongly dependent on the net charge of the substrate (Figure 3), dropping sharply as the charge is changed from  $-2e$  (that of oxaloacetate) to  $+2e$ . A more important result is that

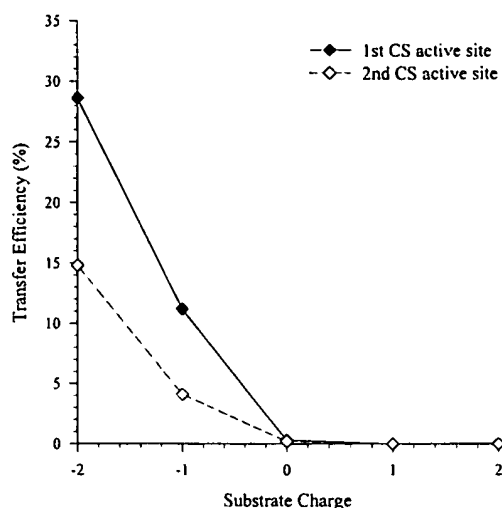


FIGURE 3: Dependence of substrate transfer efficiency on substrate charge at zero ionic strength. Transfer efficiency is defined here as the percentage of substrate molecules leaving the MDH active site which reach a CS active site.

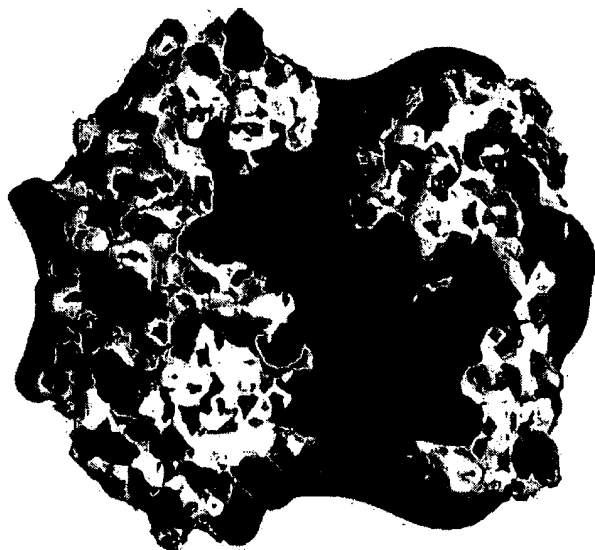


FIGURE 4: Electrostatic isopotential contours around the MDH-CS fusion protein (calculated at zero ionic strength) viewed from the same position as in Figure 2. The blue surface connects all points having a potential of +1.5 kT; the red surface connects all points having a potential of -1.5 kT. Note the presence of a continuous region of positive electrostatic potential covering the area where the MDH and CS dimers meet.

the transfer efficiency for an uncharged substrate, which is not subject to any electrostatic channeling effects (and therefore behaves in exactly the same way as a charged substrate would with the enzyme's electrostatic field switched off), is only around  $0.5 \pm 0.4\%$ . This is perhaps what one would expect, given the relative positioning of the active sites in the model of the fusion protein (Figure 2). In contrast, the transfer efficiency for a charge of  $-2e$  is  $43 \pm 2\%$ . This result, which does not seem at all obvious from simple inspection of the model structure, represents an approximate 100-fold increase in efficiency over the simulations without electrostatic channeling effects. On the other hand, the result is less surprising when the electrostatic potential around the fusion protein is examined (Figure 4); isopotential contours marked at values of  $\pm 1.5$  kT indicate

the presence of a large area of positive (i.e., favorable) electrostatic potential extending over the region where MDH and CS meet. That the transfer efficiency does not exceed 50% appears to be due to the fact that the region of favorable potential does not quite extend to the substrate starting positions, though the apparently unfavorable positioning of the MDH active site probably also plays a role. Once substrate molecules reach the region of favorable electrostatic potential however, they are likely to remain within it and, once trapped in this way, stand a good chance of ultimately diffusing to one or other of the CS active sites.

Simulations performed to assess the relative contributions of the two enzymes in determining the efficiency of substrate transfer suggest that both play important roles, though CS dominates. When the electrostatic field due only to MDH is switched off (i.e., when all atomic charges on MDH are set to zero), the transfer efficiency is reduced by a factor of 4 to  $12 \pm 2\%$ ; when the electrostatic field due only to CS is switched off, the transfer efficiency is reduced even more dramatically, to only  $0.6 \pm 0.5\%$ . This apparent dominance of CS's electrostatic field was further emphasized by the results of simulations run in the opposite direction, i.e., starting at the CS active site and terminating at the MDH active sites. In the DHFR-TS system such "backward" simulations were of comparable efficiency to the "forward" results, suggesting that in DHFR-TS the role of electrostatics is more one of restricting the substrate's diffusion to the region between the active sites than one of actively guiding substrate from one active site to the other (Elcock *et al.*, 1996). Results for the MDH-CS system are more difficult to interpret since all backward trajectories remained trapped indefinitely at the CS active site, making it impossible to calculate substrate transfer efficiencies. However, since this trapping results from strong electrostatic effects (no trapping was observed when the enzyme's electrostatic field was switched off), it is tempting, and perhaps not unreasonable, to interpret this result as implying that, in contrast to DHFR-TS, the electrostatic channeling in the MDH-CS system is indeed directional.

Consistent with the above results suggesting the importance of electrostatic effects, the transfer efficiency obtained from the simulations is found to be strongly dependent on the ionic strength of the solution (Figure 5); at 150 mM the efficiency drops to a value of  $11 \pm 2\%$ . Again, this result is understandable in terms of the electrostatic potential (Figure 6); the increased shielding of the fusion protein's charged residues means that the regions of favorable electrostatic potential no longer extend out so far into solution so that the probability of substrate escape is increased.

In the model that we have constructed substrate molecules start their trajectories at one end of the fusion protein (Figure 2). Since it is possible for the substrate to diffuse from this position around either side of the protein, reactions are expected to be obtained at both of the CS active sites. However, as the substrate starting positions are slightly displaced toward one side of the protein, it is perhaps not surprising that an approximately 2-fold preference is obtained for reaction at one of the CS active sites (from here on, we use "first" active site to mean "more favored") (Figures 3 and 5). More interesting is the fact that the distributions of reaction times (i.e., trajectory lengths) for reactions at the two CS active sites are very different (Figure 7). For the less-favored CS active site, the probability of a particular

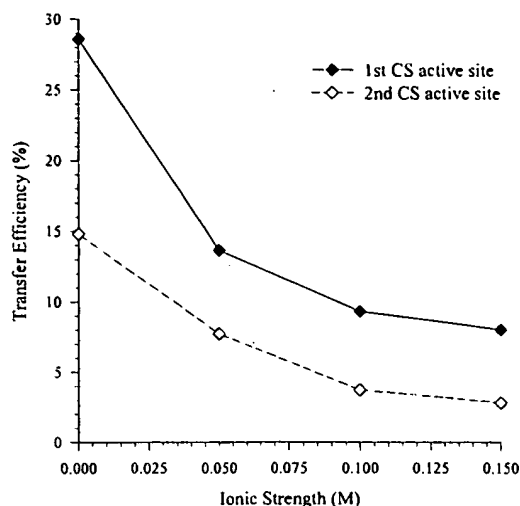


FIGURE 5: Dependence of substrate transfer efficiency on ionic strength for a substrate charge of  $-2$ .

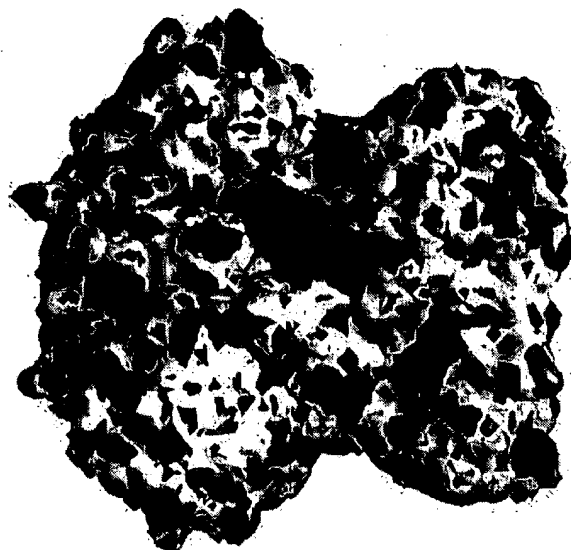


FIGURE 6: Electrostatic isopotential contours around the MDH-CS fusion protein (calculated at 150 mM) viewed from the same position as in Figure 2. The blue surface connects all points having a potential of  $+1.5$  kT; the red surface connects all points having a potential of  $-1.5$  kT.

reaction time increases monotonically as a function of the reaction time itself. In contrast, for the more favored CS active site, a distinct maximum in the distribution is observed at much shorter times, superimposed on a trend similar to that seen with the second CS active site (Figure 7). In other words, a considerable proportion of the reactive trajectories for the first CS active site reacts *very* rapidly: out of 438 trajectories which terminate at the first CS active site, 113 (26%) do so in less than 10 ns, whereas only 4 out of 227 reactive trajectories (2%) at the second CS active site react within this time. The reasons for this dramatic difference are not immediately obvious, but it is interesting to note that no correlation appears between the substrate's starting position and either its eventual fate or its speed of reaction; any concern that the results might be very sensitive to the former aspect can therefore be ruled out. Instead, it appears likely that the bimodal distribution reflects real differences in substrate trajectories, though it is by no means clear of course whether these effects will ultimately be of much

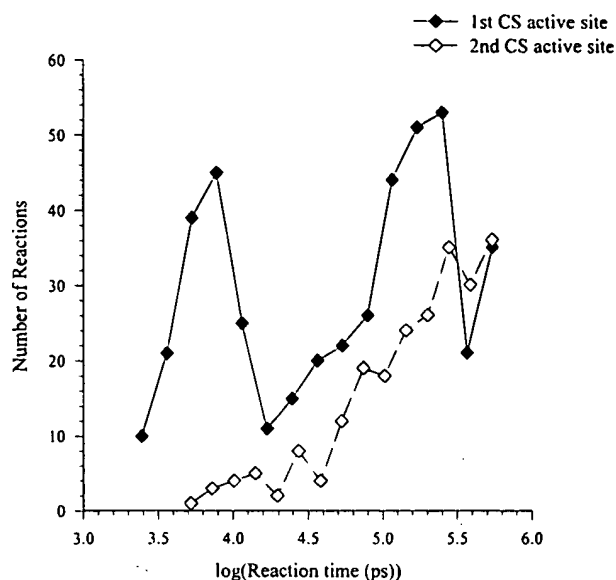


FIGURE 7: Distribution of reaction times (i.e., trajectory lengths) for reaction at the two CS active sites obtained at zero ionic strength.

relevance to overall channeling efficiency; further work will be required to address this problem more closely.

## DISCUSSION

The simulation results reported here provide evidence that the experimental observation of efficient substrate channeling in the MDH-CS fusion protein is due to an electrostatic mechanism. Since electrostatic effects appear so important in the simulations, it is of course no surprise to find that if channeling is very efficient for a substrate charge of  $-2e$  (as it is here), it is extremely inefficient for a substrate charge of  $+2e$ . On the other hand, comparison with results obtained for a substrate charge of zero is more illuminating since it gives not only a measure of the increase in transfer efficiency that might result from electrostatic channeling but also an indication of whether electrostatic channeling is required at all in the first place. In the present case, the MDH and CS active sites are separated by around 60 Å, and in the absence of electrostatic effects (i.e., when the substrate has a charge of zero) much less than 1% of substrate molecules leaving the MDH active site reach the CS active site. The simulations suggest therefore that efficient channeling of substrate does not result simply from the proximity of the CS and MDH active sites. When electrostatic effects are included however (i.e., when the substrate has a charge of  $-2e$ ), the transfer efficiency not only increases by around 2 orders of magnitude but also approaches a value that is more consistent with the experimental observation of efficient substrate channeling.

Many of the results reported here for the MDH-CS system parallel those we obtained previously in our studies of channeling in DHFR-TS (Elcock *et al.*, 1996) and are obviously those to be expected of an electrostatic channeling mechanism. The ionic strength dependence of transfer efficiency obtained here appears more marked than in our study of the DHFR-TS system, but not surprisingly follows the same qualitative trend: increasing ionic strength tends to suppress any electrostatic channeling effect which might be present. The magnitude of this ionic strength effect is likely to vary from system to system and, in extreme cases

of very strong electrostatic effects, might even be almost completely insensitive to ionic strength within the physiological range. However, in the present case it seems that ionic strength changes should result in experimentally measurable changes in the kinetics of the MDH-CS protein.

This aspect leads us to consider how contact between our theoretical findings and experimental results is to be made; it is important to stress, for example, that there is as yet no direct experimental evidence that transfer of oxaloacetate is electrostatically mediated. One problem with connecting the present work to experimental results is the use here of pig heart enzyme structures, when the experimental work involved the yeast forms of the enzymes. As stated in the introduction, this difference is unavoidable owing to the lack of structural information for the yeast enzymes. A related difficulty involves our overall structure of the fusion protein; in the absence of further structural information we have no way of knowing whether our structure represents a good or poor model of the real fusion protein. Before dismissing the results reported here as artifacts of our modeled structure however, it should be borne in mind that it places the MDH active site facing away from CS and thus would not be expected to bias the results toward very efficient channeling. A more fundamental problem, and one of obvious importance, is how to connect the transfer efficiencies obtained by simulation with lag times and other observables obtained by experimental kinetics studies. Preliminary results (unpublished work) based on a reaction kinetics scheme suggest that the transfer efficiency of ~45% obtained in our simulations is probably sufficient to account for the channeling of oxaloacetate observed in the AAT competition experiments (Lindblah *et al.*, 1994). The development of a more complete method for connecting theoretical and experimental results, which will clearly be essential for example for interpreting ionic strength effects, will form the subject of further work.

Irrespective of how directly our findings can be compared to experimental results, the 100-fold increase in transfer efficiency obtained by changing the substrate charge from 0 to  $-2e$  in our simulations argues strongly that electrostatics may be of importance for the MDH-CS system. It is interesting therefore to ask whether such a mechanism is also likely to operate elsewhere in the citric acid cycle, particularly in view of the fact that all of the cycle's substrates (intermediates) have a charge of  $-2e$  or  $-3e$ . The existence of a multienzyme complex (metabolon) formed by enzymes of the citric acid cycle has been known for some years (Barnes & Weitzman, 1986), though it remains poorly characterized (Robinson *et al.*, 1987). From a simulation point of view, interesting extensions of this work would involve investigating the two enzymes bracketing MDH and CS in the citric acid cycle, namely, fumarase and aconitase. High-resolution structures are available for both enzymes, but further information would be required before further theoretical work would be justified: in the absence of additional structural constraints, the large number of possible relative orientations of the enzymes would preclude meaningful study.

While the options for further theoretical study of channeling effects in multienzyme complexes are limited by the requirement for good structural information, experimental studies, such as kinetics measurements, suffer from no such limitation. However, in the absence of structural data, the

interpretation of the experimental results may well be difficult. It is important to point out for example that in studies in which two enzymes, which would otherwise remain separate, are forced to associate [for example by the use of a covalent linker as in the work of Lindblah *et al.* (1994)] it may not be possible to decide with certainty whether the absence of a channeling effect is real or simply due to the fact that structural constraints force the enzymes to adopt a relative orientation unfavorable for channeling. By the same token, the efficient channeling obtained in the MDH-CS fusion protein might conceivably result from the enzymes being forced to adopt a relative orientation which just happens to be favorable for channeling. In the citric acid cycle metabolon itself, the two enzymes will probably be oriented in a different way, which may either increase or decrease the efficiency of channeling.

Finally it is worth pointing out that, even if accurate structural data are available, the simulation results reported here indicate that simple inspection of a structure may not be a good guide to estimating the efficiency of substrate channeling. If an electrostatic mechanism is important, as is suggested strongly by the present results, the spatial proximity of active sites need not correlate at all with the substrate transfer efficiency; what is likely to be more important is the presence of an unbroken electrostatically favorable region connecting the active sites.

## ACKNOWLEDGMENT

A.H.E. is very grateful to Drs. Debbie L. Benson and Gary A. Huber for valuable discussions.

## REFERENCES

- Antosiewicz, J., McCammon, J. A., Wlodek, S., & Gilson, M. K. (1995) *Biochemistry* 34, 4211–4219.
- Barnes, S. J., & Weitzman, P. D. J. (1986) *FEBS Lett.* 201, 267–270.
- Brooks, B. R., Brucoleri, R. E., Olafson, B. D., States, D. J., Swaminathan, S., & Karplus, M. (1983) *J. Comput. Chem.* 4, 187–217.
- Easterby, J. S. (1973) *Biochim. Biophys. Acta* 293, 552–558.
- Elcock, A. H., Potter, M. J., Matthews, D. A., Knighton, D. R., & McCammon, J. A. (1996) *J. Mol. Biol.* (in press).
- Ermak, D. L., & McCammon, J. A. (1978) *J. Chem. Phys.* 69, 1352–1360.
- Gleason, W. B., Fu, Z., Birktoft, J., & Banaszak, L. (1994) *Biochemistry* 33, 2078–2088.
- Honig, B., & Nicholls, A. (1995) *Science* 268, 1144–1149.
- Knighton, D. R., Kan, C.-C., Howland, E., Janson, C. A., Hostomska, Z., Welsh, K. M., & Matthews, D. A. (1994) *Nat. Struct. Biol.* 1, 186–194.
- Lindblah, C., Rault, M., Hagglund, C., Small, W. C., Mosbach, K., Bülow, L., Evans, C., & Srere, P. A. (1994) *Biochemistry* 33, 11692–11698.
- Mackerell, A. D., Wiórkiewicz-Kuczera, J., & Karplus, M. (1995) CHARMM22 parameter set, Department of Chemistry, Harvard University, Oxford St., Cambridge, MA.
- Madura, J. D., Davis, M. E., Gilson, M. K., Wade, R. C., Luty, B. A., & McCammon, J. A. (1994) *Rev. Comput. Chem.* 5, 229–267.
- Madura, J. D., Briggs, J. M., Wade, R. C., Davis, M. E., Luty, B. A., Ilin, A., Antosiewicz, J., Gilson, M. K., Bagheri, B., Scott, L. R., & McCammon, J. A. (1995) *Comput. Phys. Commun.* 91, 57–95.
- Meek, T. D., Garvey, E. P., & Santi, D. V. (1984) *Biochemistry* 24, 678–686.
- Nicholls, A., Sharp, K., & Honig, B. (1991) *Proteins* 11, 281–296.

QUANTA version 4.0 (1994) Molecular Simulations Inc., 200 Fifth Ave., Waltham, MA.  
Reed, L. J. (1974) *Acc. Chem. Res.* 7, 40–46.  
Remington, S., Wiegand, G., & Huber, R. (1982) *J. Mol. Biol.* 158, 111–152.  
Srere, P. A. (1985) *Trends Biochem. Sci.* 10, 109–110.  
Stroud, R. M. (1994) *Nat. Struct. Biol.* 1, 131–134.

Trujillo, M., Donald, R. G. K., Roos, D. S., Greene, P. J., & Santi, D. V. (1995) *FASEB J.* 9, A1337.  
Trujillo, M., Donald, R. G. K., Roos, D. S., Greene, P. J., & Santi, D. V. (1996) *Biochemistry* 35, 6366–6374.  
Welch, G. R. (1977) *Prog. Biophys. Mol. Biol.* 32, 103–191.  
BI9614747



## Construction of a homodimeric dihydrofolate reductase–thymidylate synthase bifunctional enzyme

M.Trujillo, R.Duncan and D.V.Santi<sup>1</sup>

Department of Biochemistry and Biophysics and Department of Pharmaceutical Chemistry, University of California, San Francisco, CA 94143-0448, USA

<sup>1</sup>To whom correspondence should be addressed

A gene encoding a bifunctional homodimeric dihydrofolate reductase–thymidylate synthase (DHFR–TS) was constructed by destroying the stop codon of *Escherichia coli* dihydrofolate reductase (DHFR) and joining the coding sequences of the monofunctional enzymes by a five amino acid linker. The protein was designed to mimic features of active site proximity and electrostatics in the protozoan DHFR–TSs which are believed to be important in channeling of the DHFR substrate, H<sub>2</sub>folate, to TS. The genetically engineered catalytically active homodimeric bifunctional DHFR–TS was expressed, purified and characterized. The component activities of the purified bifunctional enzyme had kinetic properties similar to those of the monofunctional TS and DHFR, but unlike the authentic bifunctional enzymes from protozoa this enzyme did not kinetically channel dihydrofolate from DHFR to TS.

**Keywords:** bifunctional DHFR–TS/engineered DHFR–TS/linker/kinetic channeling/substrate channeling.

### Introduction

Thymidylate synthase (TS; EC 2.1.1.45) and dihydrofolate reductase (DHFR; EC 1.5.1.3) catalyze sequential reactions in the *de novo* synthesis of thymidine-5'-monophosphate (dTMP) (Figure 1). TS catalyzes the reductive methylation of 2'-deoxyuridine-5'-monophosphate (dUMP) by 5,10-methylene-5,6,7,8-tetrahydrofolate (CH<sub>2</sub>H<sub>4</sub>folate) to produce dTMP and 7,8-dihydrofolate (H<sub>2</sub>folate), and DHFR catalyzes the subsequent NADPH-dependent reduction of H<sub>2</sub>folate to generate 5,6,7,8-tetrahydrofolate (H<sub>4</sub>folate). Both TS and DHFR exist as distinct, monofunctional enzymes in sources as varied as bacteriophage, bacteria, fungi, viruses and mammals (Ackermann and Potter, 1949; Blakley, 1984). In most genera, TS is a dimer of identical subunits of about 35 kDa (Carreras and Santi, 1995) whereas monofunctional DHFR is a monomer of about 20 kDa (Blakley, 1984). In contrast, TS and DHFR exist on the same polypeptide chain in protozoa (Ivanetich and Santi, 1990) and higher plants (Lazar *et al.*, 1993). The bifunctional protein is a dimer of identical subunits with an N-terminal DHFR domain connected to a TS domain by a linker of variable length depending on the source of the enzyme.

Substrate channeling has been proposed as a biological advantage of bifunctional DHFR–TSs over their monofunctional counterparts (Meek *et al.*, 1985). Kinetic evidence for substrate channeling of the H<sub>2</sub>folate produced by TS to the DHFR active site has been reported for the *Leishmania major* and *Toxoplasma gondii* DHFR–TSs (Meek *et al.*, 1985; Trujillo *et al.*, 1996), but the mechanism of channeling remains

unknown. It is possible that the channeling of H<sub>2</sub>folate in the bifunctional proteins occurs because of the proximity of the TS and DHFR active sites that results from linkage of the domains. In this case, DHFR would simply be exposed to the higher local concentration of TS-generated H<sub>2</sub>folate before it dilutes into bulk solvent. However, from the recently reported crystal structure of *L.major* TS–DHFR, it has been suggested that the TS and DHFR sites may not be sufficiently close to permit channeling by proximity (Knighton *et al.*, 1994). Another proposed mechanism for channeling is based on the surface charge distribution of *L.major* DHFR–TS (Knighton *et al.*, 1994). The protein has surfaces of positive electrostatic potential that lie between and within the TS and DHFR domain binding sites for H<sub>2</sub>folate, and the negatively charged H<sub>2</sub>folate could be shuttled directly between the two active sites by way of electrostatic interactions. The crystal structures of the *Escherichia coli* DHFR and TS monofunctional enzymes reveal similar regions of positive charge around the active sites of the monofunctional enzymes (Stroud, 1994). Linking the monofunctional *E.coli* DHFR and TS to produce a bifunctional protein provides an approach to testing the aforementioned hypotheses for channeling. Such a protein could provide high H<sub>2</sub>folate concentrations near the DHFR site and also simulate the electrostatic environment surrounding the H<sub>2</sub>folate binding sites, although it would lack some of the electrostatic properties of protozoan bifunctional DHFR–TSs which may contribute to the proposed channeling mechanism (Knighton *et al.*, 1994). Furthermore, it has been suggested that at the high local enzyme concentrations present *in vivo* (Srere, 1987), the monofunctional enzymes might associate (Kawai and Hillcoat, 1974; Mathews *et al.*, 1988; Moen *et al.*, 1988) and also be capable of channeling H<sub>2</sub>folate (Stroud, 1994). This hypothesis could also be tested by linkage of the two monofunctional enzymes into a bifunctional protein.

Recently the coding sequences of the *E.coli* DHFR and TS were linked in an expression vector in an attempt to produce the bifunctional DHFR–TS homodimer (Iwakura and Kokubu, 1995). Upon expression, TS homodimer and TS–(DHFR–TS) heterodimer were isolated without the desired DHFR–TS homodimer. In the present paper, we describe the construction of a gene for a bifunctional *E.coli* DHFR–TS and its expression and purification as a catalytically active homodimer similar to the natural protozoan enzymes. We present the kinetics of H<sub>2</sub>folate transfer between the TS and DHFR domains of the bifunctional enzyme and report that there is no kinetic channeling of H<sub>2</sub>folate.

### Materials and methods

#### Materials

*Escherichia coli* strain DH5 $\alpha$ , obtained from BRL, was used for general manipulation of recombinant plasmids. *Escherichia coli* strain Thy<sup>–</sup>  $\chi$ 2913RecA ( $\Delta$ thyA 572, recA56) was used for expression of the engineered bifunctional DHFR–TS (Climie *et al.*, 1992). pThyA, which contains the *E.coli* TS gene

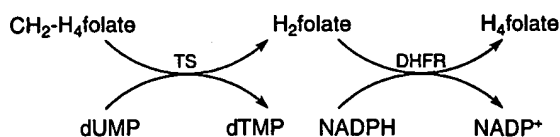


Fig. 1. The reactions catalyzed by thymidylate synthase (TS) and dihydrofolate reductase (DHFR).

in Bluescript KS (Maley and Maley, 1988), was a gift from F. Maley. The expression vector pTrc 99A, which contains the *lac* I<sup>q</sup> gene and the *trc* promoter, was purchased from Pharmacia. General methods for ligation and transformation of *E. coli* were performed as previously described (Sambrook *et al.*, 1989). Restriction endonucleases, T4 ligase and vent DNA polymerase were from New England Biolabs, Life Technologies, Inc. or Boehringer Mannheim. Oligonucleotides were synthesized at the Biomolecular Resource Center at the University of California, San Francisco, using cyanoethyl phosphoramidite chemistry. Automated DNA sequencing was performed at the Biomolecular Resource Center, University of California, San Francisco, using the Taq dye terminator cycle sequencing chemistry. CH<sub>2</sub>H<sub>4</sub>folate (Bruce and Santi, 1982), enantiomerically pure H<sub>2</sub>folate (Roos, 1993) and methotrexate (MTX)-Sephacrose CL-6B (~1 µmol MTX/ml resin) (Meek *et al.*, 1985) were prepared as described. Purified *E. coli* DHFR and *E. coli* TS were gifts of C.R. Matthews and F. Maley, respectively. Protein concentrations were determined by the Bradford method using bovine serum albumin (BSA) as a standard (Bradford, 1976). SDS-PAGE was performed as previously described (Read and Northcote, 1981).

#### Structure alignments

The UCSF MidasPlus software system from the Computer Graphics Laboratory, University of California, San Francisco, was used to obtain alignments of the crystal structures of *E. coli* TS with 5-fluoro-2'-deoxyuridine 5'-monophosphate (FdUMP) and 10-propargyl-5,8-dideazafolate (CB3717) bound (Fauman *et al.*, 1994) and *E. coli* DHFR with folate and NADP<sup>+</sup> bound (Bystroff *et al.*, 1990) to the structure of *L. major* DHFR-TS with FdUMP and CB3717 bound to the TS domains and MTX and NADPH to the DHFR domains (Knighton *et al.*, 1994). The structures were matched by means of a least-squares fit of the coordinates of the backbone  $\alpha$ -carbons of three conserved active site residues and one additional conserved residue. The backbone  $\alpha$ -carbons of the following residues were used for the TS alignment: C146, I264, E58 and L38 for *E. coli* and C400, I520, E292 and L271 for *L. major*. The backbone  $\alpha$ -carbons of the following residues were used for the DHFR alignment: G15, W22, T35 and F125 for *E. coli* and G40, W47, T60 and F193 for *L. major*. The distance between the DHFR C-terminus and the TS N-terminus of the matched monofunctional enzymes was then determined.

#### Construction of expression vector pTDDHFR-TS

The 5' end of the *E. coli* TS gene was modified by PCR using pThyA as a template. Two synthetic primers P1 (5'-ACCGCTCGAGCGTCGTTGGTGCGAGCTCTGGTGA AAAACAGTATTTAGAACTG-3') and P2 (5'-CTGGTTCAGTACCGTAGT-3') were used for the PCR amplification step. The P1 primer introduced several features: the C-terminus of the coding sequence of DHFR with the stop codon removed, a linker region and the N-terminus of the coding sequence of TS with the first methionine changed to a glutamate (underlined and bold). In addition, an *Xho*I site (underlined) for cloning

and a *Sac*I site (bold) within the linker were introduced. P2 primed in the reverse direction on the TS coding sequence downstream from the *Bss*HI site. The resulting DNA fragment was digested with *Xho*I and *Bss*HI and cloned into pThyA to yield pTD1, which was checked by restriction analysis and DNA sequencing of the amplified region.

The *E. coli* DHFR coding sequence was amplified by PCR using DH5 $\alpha$  chromosomal DNA as a template. Two synthetic primers P3 (5'-CCCCGGTACCTCATGATCAGTCTGATTGCG-3') and P4 (5'-CCGGCTCGAGAATCTCAAAGCAATAGCT-3') were used. The P3 primer introduced a *Kpn*I site (underlined) and a *Bsp*HI site (bold) at the beginning of the DHFR coding sequence. P4, which includes a unique *Xho*I site (underlined) present in the DHFR coding sequence, primed in the reverse direction two amino acids before the C-terminus of the DHFR coding sequence. The resulting DNA fragment was digested with *Kpn*I and *Xho*I and then cloned into pTD1 to give pTD2, which was checked by restriction analysis and DNA sequencing of the amplified region. pTD1 and pTD2, both of which are in Bluescript KS, do not contain ribosome binding sites. In order to achieve controlled expression of the bifunctional gene, it was necessary to transfer the construction into another vector such as pTrc 99A. Digestion of pTD2 with *Bsp*HI and *Bam*HI followed by ligation of the resulting fragment with pTrc 99A that had been restricted with *Nco*I and *Bam*HI yielded the final construction, pTDDHFR-TS.

#### Expression and purification of *E. coli* DHFR-TS

pTDDHFR-TS was transformed into *E. coli* strain Thy<sup>-</sup> x2913. A suspension of cells from 3 l IPTG-induced culture was lysed using a French press. High molecular weight nucleic acids were precipitated by the addition of streptomycin sulfate. The resulting supernatant was loaded at 4°C on a Q-Sepharose column (30 ml bed volume), which had been pre-equilibrated with buffer A (20 mM Tris-HCl pH 7.4, 1 mM EDTA and 1 mM DTT). The column was washed extensively with buffer A containing 0.3 M KCl. The protein was eluted with a 300 ml linear gradient of 0.3 to 1 M KCl in buffer A. *Escherichia coli* DHFR-TS eluted at approximately 0.7 M KCl. KCl was added to the pooled fractions to a final concentration of 1.2 M KCl. The pool was loaded at 4°C on a phenyl-Sepharose column (30 ml bed volume) that had been previously equilibrated with buffer A containing 1.2 M KCl. The protein did not bind well to the column and it was recovered in an initial wash of the column with buffer A containing 1.2 M KCl. The protein was concentrated using Centrprep-30 from Amicon to a final volume of 10 ml.

#### Enzyme assays

Thymidylate synthase activity was assayed spectrophotometrically by monitoring formation of H<sub>2</sub>folate at 340 nm ( $\epsilon_{340} = 6400 \text{ M}^{-1} \text{ cm}^{-1}$ ) in 50 mM TES (pH 7.8), 0.1 mM CH<sub>2</sub>H<sub>4</sub>folate, 0.1 mM dUMP, 75 mM 2-mercaptoethanol, 1 mM EDTA and 5 mM H<sub>2</sub>CO (Wahba and Friedkin, 1961). DHFR activity was monitored by measuring the decrease in absorbance at 340 nm resulting from consumption of H<sub>2</sub>folate and NADPH ( $\epsilon_{340} = 12300 \text{ M}^{-1} \text{ cm}^{-1}$ ) in 50 mM TES (pH 7.0), 0.1 mM H<sub>2</sub>folate, 0.1 mM NADPH, 75 mM 2-mercaptoethanol, 1 mM EDTA and 1 mg/ml BSA (Hillcoat *et al.*, 1967). For both TS and DHFR, one unit of enzyme activity is defined as the amount of enzyme that produces 1 µmol of product per minute at 25°C.

For determination of the steady-state kinetic parameters, the concentration of one substrate was varied between approxi-

mately 0.5 and 10  $K_m$ , with the other substrate fixed at 100  $\mu$ M. The  $K_m$  value for  $H_2$ folate was determined using a 10 cm cuvette. Kinetic constants were calculated from a non-linear square fit to the Michaelis-Menten equation using Kaleidagraph (Abelbeck Software) on a Macintosh computer.

Inhibition of DHFR by pyrimethamine (Pyr) was measured by varying the concentration of inhibitor in a reaction mixture containing 4.3 nM enzyme and 10  $\mu$ M  $H_2$ folate. The  $K_i$  was calculated using the equation for competitive inhibition from Segel (Segel, 1975).

#### Coupled assay

The DHFR-TS coupled system was assayed by monitoring the decrease in NADPH absorbance at 340 nm in the absence of added  $H_2$ folate (Meek *et al.*, 1985). The assay mixture containing 28  $\mu$ M  $CH_2H_4$ folate and 30  $\mu$ M NADPH in 50 mM TES (pH 7.8), 75 mM 2-mercaptoethanol, 1 mM EDTA, 5 mM  $H_2CO_3$ , 1 mg/ml BSA and variable amounts of enzyme was incubated at room temperature until no change in absorbance at 340 nm was detectable. In this assay the formaldehyde reacts with  $H_4$ folate to regenerate  $CH_2H_4$ folate, which makes the assay cyclic. The reaction was initiated by addition of 25  $\mu$ l of 8 mM dUMP (final concentration 200  $\mu$ M), and the decrease in absorbance was monitored at 340 nm ( $\epsilon_{340} = 5900$  M<sup>-1</sup> cm<sup>-1</sup>).

In addition, individual TS and DHFR rates of the bifunctional enzyme were determined under conditions of the coupled assay, with the following modifications: for DHFR, dUMP was omitted and 100  $\mu$ M  $H_2$ folate was included; for TS, NADPH was omitted.

#### Analytical gel filtration

Gel filtration of *E. coli* DHFR-TS was performed on a Superose 12HR 10/30 column. One hundred  $\mu$ l of the purified enzyme (1 mg/ml) in buffer A containing 1.2 M KCl was injected, and the column was eluted with buffer A at a flow rate of 0.5 ml/min. The column was calibrated with molecular weight standards of 43 to 2000 kDa.

## Results

#### Structure alignments

The monofunctional crystal structures of *E. coli* TS (Fauman *et al.*, 1994) and *E. coli* DHFR (Bolin *et al.*, 1982) were matched to that of *L. major* DHFR-TS (Knighton *et al.*, 1994) using the UCSF MidasPlus program. The alignment of the TS domains yielded a root mean square error of 0.42 Å and that of the DHFR domains gave an error of 0.67 Å. A similar alignment of the monofunctional *E. coli* enzymes with the *L. major* protein has been performed by Stroud (see Figure 2 of Stroud, 1994) who compared the electrostatic potential obtained for the *E. coli* enzymes to that obtained by Knighton for the *L. major* DHFR-TS (see Figure 6 of Knighton *et al.*, 1994).

The interface of the matched *E. coli* structures is shown in Figure 2 along with that of the *L. major* bifunctional enzyme. The fit of the two surfaces was achieved by choosing different side chain rotomers of some interface residues. In this model, there are no steric clashes or polarity problems apparent between sidechains of the two monofunctional enzymes. Two sets of surface sidechains of opposite polarity are close enough together that it would be possible for them adopt conformations that would permit charge interactions across the interface (DHFR D157 with TS R225 and DHFR K109 with TS D253).

The modelled distance between the monofunctional DHFR

C-terminus and the monofunctional TS N-terminus was determined to be about 10 Å. A linker composed of five amino acids (GASSG) was used to connect the monofunctional *E. coli* DHFR and TS enzymes (Figure 3). The distance between the C- and N-terminus of the linker in its fully extended conformation was about 18 Å, which is sufficiently long to allow the engineered *E. coli* DHFR-TS bifunctional enzyme to adopt the structure of the *L. major* bifunctional enzyme.

#### Construction of expression vector pTDDHFR-TS

The *E. coli* bifunctional DHFR-TS gene was successfully cloned under the control of the inducible *trc* promoter in pTrc 99A. The gene includes the coding sequence for *E. coli* DHFR with the stop codon removed, the coding sequence for the linker region and the coding sequence of *E. coli* TS with the TS starting methionine changed to a glutamate. This amino acid was selected because all TSs have either a starting methionine or an acidic residue at this position.

#### Expression and purification of *E. coli* DHFR-TS

Crude extracts of IPTG induced cultures containing pTDDHFR-TS were analyzed by SDS-PAGE. A protein band representing ~10% of the total soluble protein was detected which migrated with a molecular mass of 48 kDa, the predicted size of the bifunctional protein. The soluble crude extract showed TS and DHFR activities of 0.08 U/mg and 0.1 U/mg, respectively, whereas no TS activity was detectable in the control crude extract from cells harboring pTrc 99A.

Initial attempts to purify the bifunctional protein using a MTX-Sepharose column were unsuccessful. The protein bound very tightly and could only be eluted by 0.01 M NaOH, which destroyed its activity. Instead, the *E. coli* DHFR-TS was purified by treatment of the crude extract with streptomycin sulfate followed by sequential chromatography on Q-Sepharose and phenyl-Sepharose columns. A total of 16 milligrams of apparently homogeneous protein was obtained (Figure 4), with TS and DHFR activities of 1.1 U/mg and 2.5 U/mg, respectively.

#### Characterization of *E. coli* DHFR-TS

The purified enzyme migrated as a single 48 kDa band on SDS-PAGE (Figure 4). It eluted from Superose 12HR 10/30 with an apparent molecular mass of ~100 kDa, indicating that the native protein was a dimer of identical subunits.

Kinetic parameters for DHFR and TS were determined for the bifunctional protein (Table I). The  $K_m$  value for DHFR was 2.0  $\mu$ M for  $H_2$ folate and the  $k_{cat}$  was 32 s<sup>-1</sup>. The  $K_m$  value for TS was 4.3  $\mu$ M for  $CH_2H_4$ folate and the  $k_{cat}$  was 1.0 s<sup>-1</sup>. The  $IC_{50}$  value for Pyr was determined in a reaction containing 10  $\mu$ M  $H_2$ folate. The  $K_i$  was calculated to be 47 nM. These parameters are similar to those previously reported for the *E. coli* monofunctional enzymes (Stone and Morrison, 1986; Howell *et al.*, 1990; Zapf *et al.*, 1993).

#### Coupled assay

A previously described coupled assay system (Meek *et al.*, 1985) was used to monitor the DHFR-catalyzed reduction of the  $H_2$ folate formed by TS. The DHFR-catalyzed reaction converts NADPH to NADP<sup>+</sup>, and the resulting decrease in the concentration of NADPH can be monitored at 340 nm. Under steady state conditions, Equation 1 describes the time course of NADP<sup>+</sup> formation (Easterby, 1973; Rudolph *et al.*, 1979; Meek *et al.*, 1985).

$$[NADP^+] = v_1 t + (v_1/v_2) K_m (e^{-v_2 t/K_m} - 1) \quad (1)$$

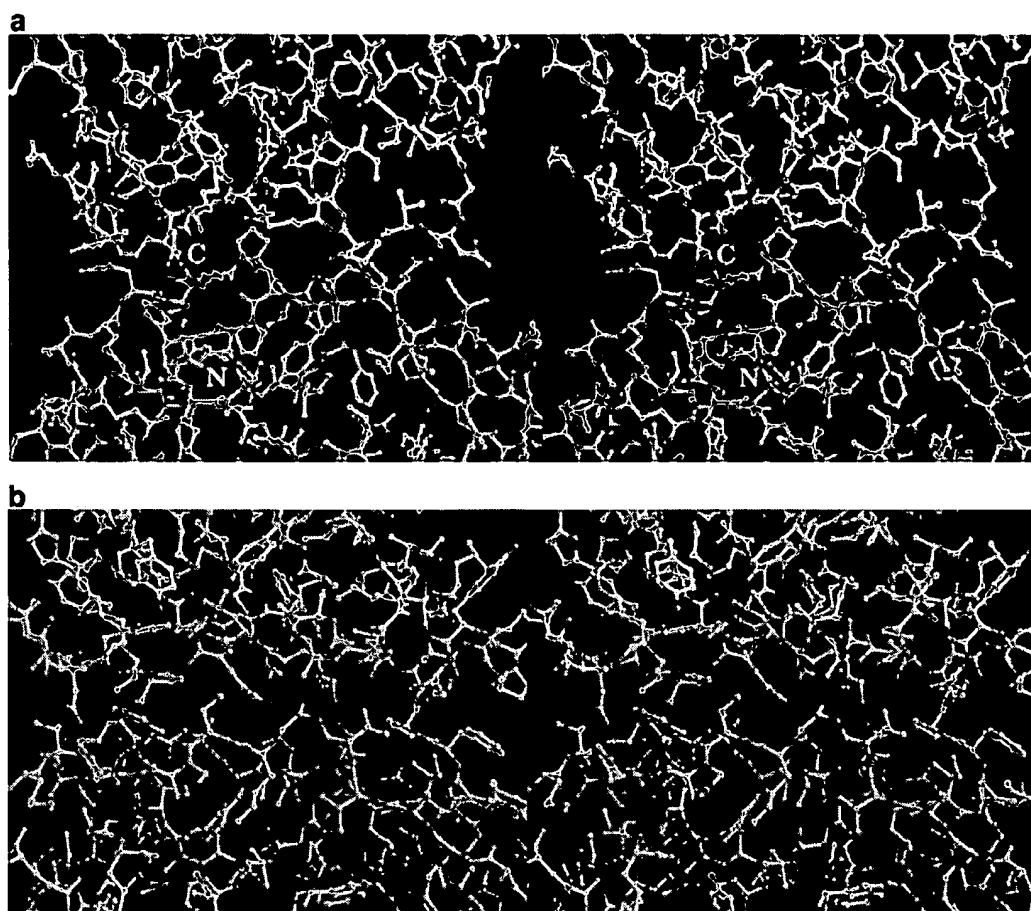


Fig. 2. (a) Stereoscopic image of the interface of *E. coli* DHFR and TS. DHFR is shown in green, and TS is shown in purple. The C-terminus of DHFR and the N-terminus of TS are labeled. The structures of the monofunctional enzymes were aligned as described in the text. The structures are as described (Bolin *et al.*, 1982; Fauman *et al.*, 1994) except that different sidechain rotomers of some surface residues have been chosen to avoid steric clash (DHFR Q108, D87, E134 and R158 and TS E250 and E223). (b) Stereoscopic image of the interface of *L. major* DHFR and TS shown for comparison.

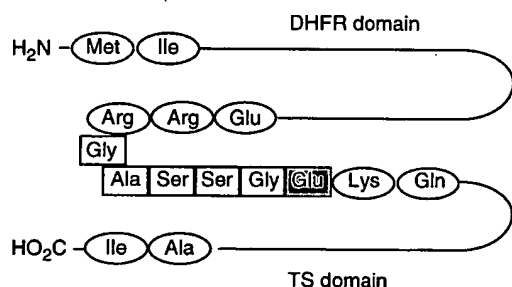


Fig. 3. Engineered bifunctional *E. coli* DHFR-TS with linker (empty boxes). The first methionine of wild-type TS was changed to a glutamate (shaded box).

In this equation,  $K_m$  is the  $K_m$  for  $H_2^{folate}$ ,  $v_1$  is the rate of TS under conditions of the coupled assay, and  $v_2$  is the rate of DHFR under near-saturating concentrations of substrates. In a plot of  $[NADP^+]$  versus time, extrapolation of the linear portion of the curve to the horizontal axis provides the lag time ( $K_m/v_2$ ) that precedes attainment of the steady-state concentration of  $H_2^{folate}$  and extrapolation to the vertical axis provides the steady-state concentration ( $v_1 K_m/v_2$ ) of  $H_2^{folate}$ . In a coupled assay in which the two enzymes do not channel

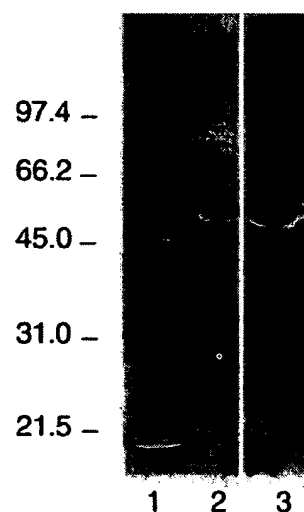


Fig. 4. SDS-PAGE gel showing purification of the recombinant *E. coli* DHFR-TS. Lane 1, crude extract; lane 2, Q-Sepharose pool; lane 3, phenyl-Sepharose pool.

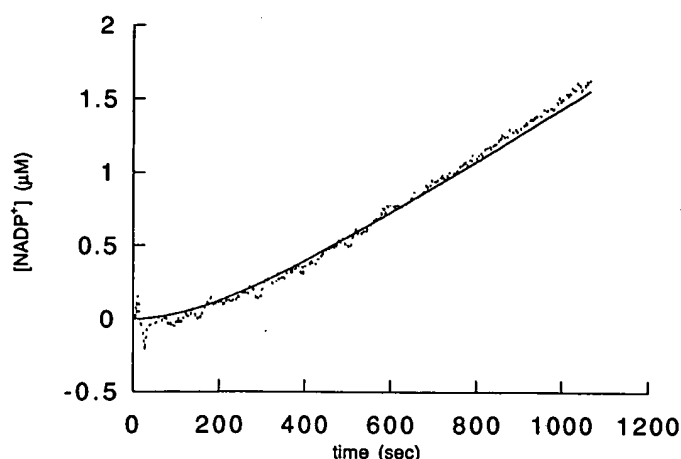


Fig. 5. Time course for  $\text{NADP}^+$  formation in the coupled assay using the bifunctional *E. coli* DHFR-TS. The dashed line represents the observed time course and the solid line represents the calculated one based on Equation 1. In this experiment, the rate of TS was  $0.11 \mu\text{M}/\text{min}$  and that of DHFR was  $0.55 \mu\text{M}/\text{min}$ .

Table I. Summary of DHFR and TS kinetic parameters

Enzyme	DHFR activity			TS activity	
	$k_{\text{cat}}$ ( $\text{s}^{-1}$ )	$K_m$ ( $\mu\text{M}$ ) for $\text{H}_2\text{folate}$	$K_i$ (nM) for Pyr	$k_{\text{cat}}$ ( $\text{s}^{-1}$ )	$K_m$ ( $\mu\text{M}$ ) for $\text{CH}_2\text{H}_4\text{folate}$
DHFR-TS	32	2.0	47	1.0	4.3
Wild-type DHFR	29 <sup>a</sup>	1.1 <sup>a</sup>	10 <sup>b</sup>	NA <sup>c</sup>	NA <sup>c</sup>
Wild-type TS	NA <sup>c</sup>	NA <sup>c</sup>	NA <sup>c</sup>	3.7 <sup>d</sup>	19 <sup>d</sup>

<sup>a</sup>Howell *et al.*, 1990.

<sup>b</sup>Stone and Morrison, 1986.

<sup>c</sup>NA, not applicable.

<sup>d</sup>Zapf *et al.*, 1993.

Table II. Coupled assay using a mixture of monofunctional *E. coli* TS and DHFR and the bifunctional *E. coli* DHFR-TS homodimer

	Rate ( $\mu\text{M}/\text{min}$ )		Lag time (s)		Steady-state [ $\text{H}_2\text{folate}$ ] ( $\mu\text{M}$ )	
	TS	DHFR	Calc.	Exp.	Calc.	Exp.
Bifunctional DHFR-TS	0.11	0.55	218	217	0.40	0.43
Monofunctional DHFR + TS	0.53	1.43	126	150	1.11	1.14

the intermediate substrate, the experimentally determined lag time and steady-state  $\text{H}_2\text{folate}$  concentration will match those values calculated using Equation 1, while in an assay in which the enzymes do channel, both values will be reduced from those calculated using Equation 1.

The coupled assay was first performed using a mixture of the monofunctional *E. coli* enzymes, such that the TS rate was  $0.53 \mu\text{M}/\text{min}$  and the DHFR rate was  $1.43 \mu\text{M}/\text{min}$  (Table II). The experimentally determined values of 150 s for the lag time and  $1.14 \mu\text{M}$  for the steady-state concentration of  $\text{H}_2\text{folate}$  are similar to those calculated using Equation 1 (126 s and  $1.11 \mu\text{M}$ , respectively), confirming the validity of the equation under our experimental conditions for a non-channeling system. As a control for a channeling system, the bifunctional DHFR-TS from *T. gondii* (Trujillo *et al.*, 1996) was used in the same assay; in that case the lag time was below our detection limit of about 20 s (data not shown) indicating that  $\text{H}_2\text{folate}$  channels

between the enzyme's TS and DHFR active sites. The coupled assay was then carried out with the *E. coli* bifunctional DHFR-TS, using a preparation of the enzyme in which the TS rate was  $0.11 \mu\text{M}/\text{min}$  and the DHFR rate was  $0.55 \mu\text{M}/\text{min}$  (Figure 5). In this case, both the experimentally determined and the calculated lag times were about 220 s, suggesting that there was no kinetic channeling of  $\text{H}_2\text{folate}$  from the active site of TS to that of DHFR. The experimentally observed steady-state concentration of  $\text{H}_2\text{folate}$  of  $0.43 \mu\text{M}$  was essentially the same as the calculated value of  $0.40 \mu\text{M}$ , confirming that the fusion of the DHFR and TS enzymes does not affect the rate of  $\text{H}_2\text{folate}$  transfer between the two active sites.

## Discussion

It has been shown that both the *L. major* and *T. gondii* bifunctional DHFR-TSs channel the intermediate,  $\text{H}_2\text{folate}$ , between the TS and DHFR active sites of the enzymes (Meek *et al.*,

1985; Trujillo *et al.*, 1996). In the crystal structure of the *L. major* protein, the active sites within a subunit are separated by a distance of about 40 Å and those on opposite subunits are separated by about 70 Å (Knighton *et al.*, 1994). Knighton and colleagues suggested that both distances appear to be too long to allow channeling of the intermediate on the basis of proximity. They proposed that a possible driving force for channeling of H<sub>2</sub>folate could be electrostatic interactions between the negatively charged intermediate and the numerous positively charged patches on the surface of the protein. Stroud then noted that alignment of the structures of monofunctional *E. coli* TS and DHFR with that of the *L. major* bifunctional enzyme revealed similar areas of positive potential (Stroud, 1994). He suggested that *E. coli* TS and DHFR might be capable of channeling H<sub>2</sub>folate at the high local enzyme concentrations present *in vivo* either through the proposed electrostatic pathway or by way of a hinging mechanism which would allow the active sites to approach each other. An approach to testing this hypothesis is to join *E. coli* DHFR and TS via an appropriate linker and to determine whether the resulting engineered bifunctional protein channels H<sub>2</sub>folate.

In a recent study by Iwakura and Kokubu, the *E. coli* monofunctional DHFR and TS enzymes were joined by a short peptide linker which included a ribosome binding site (Iwakura and Kokubu, 1995). Because the TS gene was preceded by a ribosome binding site and because it contained a start codon, they obtained a mixture of products that included heterodimeric bifunctional TS–(DHFR–TS), homodimeric monofunctional TS and an intractable aggregated form of bifunctional DHFR–TS. Studies of the heterodimeric TS–(DHFR–TS) did not permit definitive conclusions to be drawn regarding kinetic channeling between the TS and DHFR sites.

In the present study, a fully active homodimeric bifunctional *E. coli* DHFR–TS was constructed by connecting the monofunctional *E. coli* enzymes via a five amino acid long linker. The linker was designed to allow the engineered *E. coli* bifunctional DHFR–TS the possibility of adopting the conformation of the *L. major* bifunctional enzyme. The 18 Å length of the fully extended linker was more than sufficient to span the necessary modeled 10 Å distance. In addition, the linker was made flexible by the presence of glycines and soluble by the presence of serines (Robinson and Sauer, 1996). Expression and purification provided the desired homodimeric bifunctional protein with a subunit molecular weight of about 48 kDa and both TS and DHFR activities. Steady-state kinetic parameters of the individual enzymes of the bifunctional protein were similar to those observed for the wild-type monomeric *E. coli* DHFR and the dimeric *E. coli* TS.

Kinetic channeling in the *E. coli* bifunctional DHFR–TS coupled system was studied by examination of the time required for the appearance of NADP<sup>+</sup> and calculation of the steady state concentration of H<sub>2</sub>folate. For a coupled system in which there is no channeling, the lag time and the steady state concentration of intermediate can be predicted by Equation 1, while in a system that channels the experimentally determined values of both parameters will be reduced from those predicted. This approach has been used previously to demonstrate kinetic channeling of H<sub>2</sub>folate for both *L. major* and *T. gondii* DHFR–TSs (Meek *et al.*, 1985; Trujillo *et al.*, 1996). The experimentally determined lag time and the steady-state concentration of H<sub>2</sub>folate for the engineered *E. coli* TS–DHFR were similar to the values predicted for a mixture of monofunctional DHFR and TS with the same rates, indicating that the bifunctional

homodimeric DHFR–TS does not channel H<sub>2</sub>folate from the active site of TS to that of DHFR.

Because our engineered bifunctional *E. coli* DHFR–TS does not channel H<sub>2</sub>folate, we conclude that the local concentration of H<sub>2</sub>folate obtained by linking the monofunctional *E. coli* enzymes is not sufficient to promote substrate channeling. Although the *E. coli* DHFR–TS may possess some of the features of the electrostatic environment of the *L. major* enzyme, our results regarding the role of electrostatic facilitation of H<sub>2</sub>folate transfer between the active sites are inconclusive since some features which may be important in electrostatic-mediated channeling are absent in our protein. For example, a highly basic loop present in the DHFR domain of the *L. major* DHFR–TS and absent in our *E. coli* DHFR–TS has been proposed to play a role in the channeling of H<sub>2</sub>folate (Elcock *et al.*, 1996). Finally, our finding that the conversion of the *E. coli* monofunctional DHFR and TS to a bifunctional DHFR–TS does not result in kinetic channeling contradicts proposals that high concentrations of the monofunctional enzymes might facilitate substrate channeling *in vivo*.

### Acknowledgements

We thank R.T.Sauer and C.R.Robinson for helpful suggestions regarding the design of the linker, D.A.Matthews for providing the coordinates of the *L. major* bifunctional DHFR–TS, F.Maley for pThyA and wild-type *E. coli* TS, C.R.Matthews, C.Gegg, and J.O'Neill for wild-type *E. coli* DHFR and P.J.Greene, L.Liu and J.S.Finer-Moore for helpful discussions. We also thank J.S.Finer-Moore for help with Figure 2. This work was supported by National Institutes of Health Grants AI 19358, AI 32784 and CA 14394.

### References

- Ackermann, W.W. and Potter, V.R. (1949) *Proc. Soc. Exp. Biol. Med.*, **72**, 1–9.
- Blakley, R.L. (1984) In Blakley, R.L. and Benkovic, S.J. (eds) *Chemistry and Biochemistry of Folate*. John Wiley and Sons, New York. pp. 191–253.
- Bolin, J.T., Filman, D.J., Matthews, D.A., Hamlin, R.C. and Kraut, J. (1982) *J. Biol. Chem.*, **257**, 13650–13662.
- Bradford, M.M. (1976) *Anal. Biochem.*, **72**, 248–254.
- Bruice, T.W. and Santi, D.V. (1982) *Biochemistry*, **21**, 6703–6709.
- Bystroff, C., Oatley, S.J. and Kraut, J. (1990) *Biochemistry*, **29**, 3263–3277.
- Carreras, C.W. and Santi, D.V. (1995) *Annu. Rev. Biochem.*, **64**, 721–762.
- Climic, S.C., Carreras, C.W. and Santi, D.V. (1992) *Biochemistry*, **31**, 6032–6038.
- Easterby, J.S. (1973) *Biochim. Biophys. Acta*, **293**, 552–558.
- Elcock, A.H., Potter, M.J., Matthews, D.A., Knighton, D.R. and McCammon, J.A. (1996) *J. Mol. Biol.*, **262**, 370–374.
- Fauman, E.B., Rutenber, E.E., Maley, G.F., Maley, F. and Stroud, R.M. (1994) *Biochemistry*, **33**, 1502–1511.
- Hillcoat, B.L., Nixon, N.F. and Blakley, R.L. (1967) *Anal. Biochem.*, **21**, 178–189.
- Howell, E.E., Booth, C., Farnum, M., Kraut, J. and Warren, M.S. (1990) *Biochemistry*, **29**, 8561–8569.
- Ivanetich, K.M. and Santi, D.V. (1990) *Faseb J.*, **4**, 1591–1597.
- Iwakura, M. and Kokubu, T. (1995) *J. Biochem.*, **118**, 67–74.
- Kawai, M. and Hillcoat, B.L. (1974) *Cancer Res.*, **34**, 1619–1626.
- Knighton, D.R., Kan, C.C., Howland, E., Janson, C.A., Hostomska, Z., Welsh, K.M. and Matthews, D.A. (1994) *Nature Struct. Biol.*, **1**, 186–194.
- Lazar, G., Zhang, H. and Goodman, H.M. (1993) *Plant J.*, **3**, 657–668.
- Maley, G.F. and Maley, F. (1988) *J. Biol. Chem.*, **263**, 7620–7627.
- Mathews, C.K., Moen, L.K., Wang, Y. and Sargent, R.G. (1988) *Trends Biochem. Sci.*, **13**, 394–397.
- Meek, T.D., Garvey, E.P. and Santi, D.V. (1985) *Biochemistry*, **24**, 678–686.
- Moen, L.K., Howell, M.L., Lasser, G.W. and Mathews, C.K. (1988) *J. Mol. Recognit.*, **1**, 48–57.
- Read, S.M. and Northcote, D.H. (1981) *Anal. Biochem.*, **116**, 53–64.
- Robinson, C.R. and Sauer, R.T. (1996) *Biochemistry*, **35**, 109–116.
- Roos, D.S. (1993) *J. Biol. Chem.*, **268**, 6269–6280.
- Rudolph, F.B., Baugher, B.W. and Beissner, R.S. (1979) *Methods Enzymol.*, **63**, 22–42.

- Sambrook, J., Fritsch, E.F. and Maniatis, T. (1989) *Molecular Cloning: A Laboratory Manual*, 2nd edn. Cold Spring Harbor Laboratory Press, Cold Spring Harbor, NY.
- Segel, I.H. (1975) *Enzyme Kinetics: Behavior and Analysis of Rapid-Equilibrium and Steady-State Enzyme Systems*. John Wiley and Sons, New York.
- Srere, P.A. (1987) *Annu. Rev. Biochem.*, **56**, 89–124.
- Stone, S.R. and Morrison, J.F. (1986) *Biochim. Biophys. Acta*, **869**, 275–285.
- Stroud, R.M. (1994) *Nature Struct. Biol.*, **1**, 131–134.
- Trujillo, M., Donald, R.G.K., Roos, D.V., Greene, P.J. and Santi, D.V. (1996) *Biochemistry*, **35**, 6366–6374.
- Wahba, A. and Friedkin, M. (1961) *J. Biol. Chem.*, **236**, 11–12.
- Zapf, J.W., Weir, M.S., Emerick, V., Villafranca, J.E. and Dunlap, R.B. (1993) *Biochemistry*, **32**, 9274–9281.

Received August 22, 1996; revised December 18, 1996; accepted January 8, 1997

## Kinetics of the coupled reaction catalysed by a fusion protein of yeast mitochondrial malate dehydrogenase and citrate synthase

Henrik Pettersson<sup>1</sup>, Peter Olsson<sup>2</sup>, Leif Bülow<sup>2</sup> and Gösta Pettersson<sup>1</sup>

<sup>1</sup>Avdelningen för Biokemi and <sup>2</sup>Avdelningen för Tillämpad Biokemi, Kemicentrum, Lunds Universitet, Lund, Sweden

The mechanistic implications of the kinetic behaviour of a fusion protein of mitochondrial malate dehydrogenase and citrate synthase have been reanalysed in view of predictions based on experimentally determined kinetic parameter values for the dehydrogenase and synthase activities of the protein. The results show that the time-course of citrate formation from malate in the coupled reaction catalysed by the fusion protein can be most satisfactorily accounted for in terms of a free-diffusion mechanism when consideration is taken to the inhibitory effects of NADH and oxaloacetate on the malate dehydrogenase activity. The effect of aspartate aminotransferase on the coupled reaction is likewise fully consistent with that expected for a free-diffusion mechanism. It is concluded that no tenable kinetic evidence is available to support the proposal that the fusion protein catalyses citrate formation from malate by a mechanism involving channelling of the intermediate oxaloacetate.

**Keywords:** fusion protein; channelling; malate dehydrogenase; citrate synthase.

The biological significance of a channelled transfer of metabolites between sequentially operating enzymes in metabolic pathways has been a matter of great dispute [1–3]. Several authors have argued that metabolite channelling is likely to occur due to 'proximity effects' once two sequential enzymes are brought close together, e.g. through the dynamic or static formation of a bienzyme complex. Such complex formation can be anticipated to decrease the average distance between the metabolite-producing and metabolite-consuming enzymic sites, and this has been envisaged to offer catalytic advantages in the form of enhanced steady-state and/or transient reaction rates [4–6].

The significance of proximity effects in enzymic metabolite transfer processes has been experimentally probed by kinetic studies of sequential enzymes that have been covalently fused to each other by chemical modification or genetic engineering [7–10]. Particular attention has been paid to fusion proteins containing the sequential enzymes malate dehydrogenase and citrate synthase in the metabolically central citric acid cycle. A fusion protein of the yeast form of these enzymes was biosynthesized and examined by Lindblad *et al.* [11], who found that the transient lag time for product formation in the coupled reaction catalysed by the two enzymes was shorter for the fusion protein than for the free enzymes. This was taken to indicate that there is a channelled transfer of the intermediate oxaloacetate in the fusion protein, an interpretation that received support by the observation that inhibition of the coupled reaction by aspartate aminotransferase (which competes with citrate synthase for oxaloacetate) was less with the fusion protein than with the free enzymes. Similar results have later been obtained with a fusion protein of the porcine form of the enzymes [12].

**Correspondence to** G. Pettersson, Department of Biochemistry, Chemical Center, Box 124, S-221 00 Lund, Sweden. Fax: + 46 40 156418, Tel.: + 46 40 154085, E-mail: Gosta.Pettersson@biokem.lu.se

**Abbreviations:** OAA, oxaloacetate; MDH, malate dehydrogenase; CS, citrate synthase; AAT, aspartate aminotransferase.

**Enzymes:** malate dehydrogenase (EC 1.1.1.37); citrate synthase (EC 4.1.3.7); aspartate aminotransferase (EC 2.6.1.1).

(Received 30 March 2000, accepted 9 June 2000)

Unfortunately, kinetic parameter values for the malate dehydrogenase and citrate synthase activities of the fusion proteins differ somewhat from those of the free enzymes [11,12]. This leaves some uncertainty as to whether the different kinetic behaviour of the fusion protein and the free enzymes may reflect the observed differences in kinetic parameter values rather than substrate channelling. To eliminate this uncertainty, we have now performed a more detailed kinetic study of the coupled reaction catalysed by the fusion protein containing the yeast form of the enzymes. The results do not support the previous interpretation of the reaction kinetics in terms of substrate channelling, but provide clear evidence that the kinetic behaviour of the fusion protein is fully consistent with a free-diffusion mechanism of oxaloacetate transfer between the malate dehydrogenase and citrate synthase moieties of the protein.

## EXPERIMENTAL PROCEDURES

### Materials

Porcine heart mitochondrial malate dehydrogenase (MDH) and aspartate aminotransferase (AAT) were purchased from Sigma Chemicals Co. Crystals of the enzyme suspensions were collected by centrifugation and dissolved in 40 mM potassium phosphate buffer, pH 8.1, containing 0.1 mM EDTA and 0.35 mM 2-mercaptoethanesulfonic acid. Immediately before use, enzyme solutions were passed through a HiTrap desalting column, pre-equilibrated with the above phosphate buffer. Active-site concentrations of the enzymes were determined spectrophotometrically at 280 nm using an absorption coefficient of 19.8 mm<sup>-1</sup>·cm<sup>-1</sup> for MDH [13] and 65.8 mm<sup>-1</sup>·cm<sup>-1</sup> for AAT [14].

The fusion protein of yeast citrate synthase and yeast mitochondrial malate dehydrogenase was prepared according to the protocol elaborated by Srere and coworkers, as detailed for their construction and purification of the fusion protein of the porcine enzymes [12]. *Escherichia coli* strain BL21, harbouring plasmid pODC29-Cit1–3-Mdh1 containing the gene for the fusion protein, was kindly provided by them. The purified



fusion protein obtained in the final gel filtration step was precipitated with 70% ammonium sulfate and stored at  $-20^{\circ}\text{C}$ . Protein concentrations during purification were determined by the Bradford method [15]. The concentration of the fusion protein was estimated from its steady-state MDH activity in the direction of malate formation, as determined in 50 mM Tris/HCl buffer (pH 7.5) using 0.1 mM oxaloacetate and 0.1 mM NADH. 1 unit of the fusion protein is defined as the amount of protein liberating 1  $\mu\text{mol}$   $\text{NAD}^{+}$  per min under such conditions.

$\text{NAD}^{+}$  (grade I) was obtained from Boehringer Mannheim. Malate, oxaloacetate, acetyl-CoA, glutamate, aspartate, and dithionitrobenzoate were from Sigma Chemical Co.

## Methods

All kinetic experiments were carried out at  $25^{\circ}\text{C}$  in 40 mM potassium phosphate buffer, pH 8.1. The equilibrium constant for the oxidation of malate by  $\text{NAD}^{+}$  was determined by reacting 10 mM malate with 4 mM  $\text{NAD}^{+}$  in the presence of about 0.6  $\mu\text{M}$  malate dehydrogenase. The amount of NADH formed after equilibration of the reaction solution was calculated from the 340 nm absorbance changes observed, using an absorption coefficient of  $6200\text{ M}^{-1}\text{cm}^{-1}$ . The MDH activity of the fusion protein was similarly determined at 340 nm in reaction solutions containing 10 mM malate, 4 mM  $\text{NAD}^{+}$ , and 0–40  $\mu\text{M}$  oxaloacetate or 0–50  $\mu\text{M}$  NADH.

The citrate synthase (CS) activity of the fusion protein was determined using 0.1 mM acetyl-CoA, 1 mM dithionitrobenzoate, and varied concentrations of oxaloacetate (0–1 mM). Reactions were monitored at 412 nm, where the reaction product of CoA and dithionitrobenzoate shows maximum absorption ( $\epsilon = 13\,600\text{ M}^{-1}\text{cm}^{-1}$ ). The conversion of malate into citrate in the coupled reaction catalysed by the MDH and CS activities of the fusion protein (about  $90\text{ U}\cdot\text{L}^{-1}$ ) was similarly determined at 412 nm, using 10 mM malate, 4 mM  $\text{NAD}^{+}$ , 0.1 mM acetyl-CoA, and 0.4 mM dithionitrobenzoate. In experiments where the effect of AAT on the coupled reaction was examined, 4 mM glutamate and 10–1000 nM AAT were added to the reaction solution.

Kinetic parameter values were determined by nonlinear regression analysis based on the least-squares fitting method. Numerical solutions of kinetic differential equations were obtained using integration procedures of the commercial computer program MATHEMATICA.

## RESULTS

### Preparation and general properties of the fusion protein

The fusion protein of the yeast forms of malate dehydrogenase (MDH) and citrate synthase (CS) was prepared according to the protocol elaborated by Srere and coworkers [12]. The protein was purified from 30 g wet *E. coli*, and only MDH activity was measured in the purification steps. Recovered amounts (in

MDH units) of the fusion protein during purification are given in Table 1.

As previously described [11,12], the fusion protein retains malate dehydrogenase (MDH) and citrate synthase (CS) activities. These can be assayed separately, or in the coupled reaction converting malate into citrate with intermediate formation of oxaloacetate (OAA) according to the reaction scheme in Fig. 1. The concentration of free OAA in the coupled reaction can be estimated, in principle, from the inhibition of citrate formation caused by aspartate production from OAA in the presence of glutamate and aspartate aminotransferase (AAT). The corresponding reaction step is included in Fig. 1.

In this investigation, the rate behaviour of the reaction system in Fig. 1 was examined under the same conditions as those used in the kinetic experiments reported by Lindbladh *et al.* [11], i.e. at  $25^{\circ}\text{C}$  in 40 mM phosphate buffer (pH 8.1) containing 10 mM malate, 4 mM  $\text{NAD}^{+}$ , 0.1 mM acetyl-CoA and, when applicable, 4 mM glutamate.

### Malate dehydrogenase activity of the fusion protein

MDH catalysis of the reversible oxidation of malate by  $\text{NAD}^{+}$  is known to be governed by Michaelis–Menten kinetics [16] and, at fixed concentrations of the two substrates, should conform to the steady-state rate equation

$$v_1 = \frac{\alpha(1 - q[\text{OAA}][\text{NADH}])}{1 + \beta_1[\text{OAA}] + \beta_2[\text{NADH}] + \beta_3[\text{OAA}][\text{NADH}]} \quad (1)$$

$$q = \frac{1}{[\text{malate}][\text{NAD}^{+}]K_{\text{eq}}} \quad (2)$$

where  $\alpha$  stands for the reaction velocity in the absence of products.  $\beta_1$ ,  $\beta_2$ , and  $\beta_3$  represent kinetic parameters for inhibition of the reaction by the products NADH and OAA.

Figure 2 shows initial steady-state velocities ( $v_1$ ) recorded for the MDH activity of the fusion protein in the presence of 10 mM malate, 4 mM  $\text{NAD}^{+}$ , and varied concentrations of OAA. A fit of Eqn (1) to these data for  $[\text{NADH}] = 0$  gave  $\alpha = 87 (\pm 3)\text{ nmol}\cdot\text{min}^{-1}\cdot\text{U}^{-1}$  and  $\beta_1 = 0.135 (\pm 0.011)\text{ }\mu\text{M}^{-1}$ . The parameter  $\beta_2$  was similarly determined from initial velocity measurements performed in

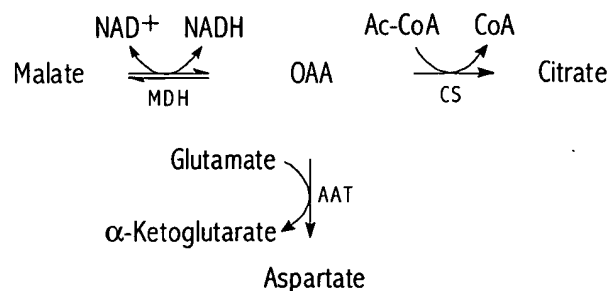


Fig. 1. Reaction system considered.

Table 1. Purification of the MDH/CS fusion protein from *E. coli* cells.

Purification step	Protein (mg)	MDH activity (U)	Specific activity ( $\text{U}\cdot\text{mg}^{-1}$ )
Sonication	1600	19 400	12
Nickel–agarose chromatography	17.2	1750	102
Gel filtration sephacryl S200	7.3	1550	213

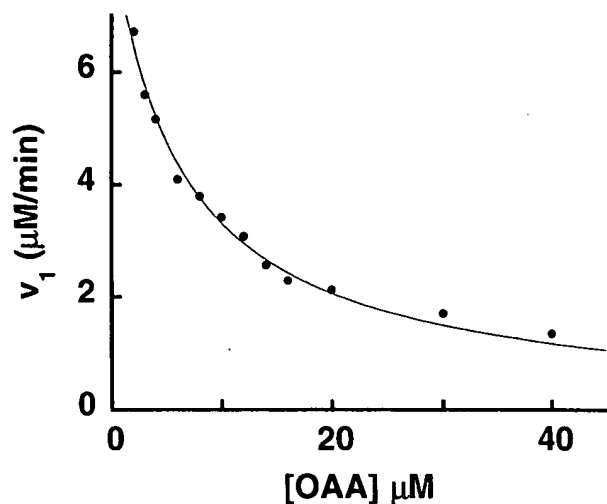


Fig. 2. MDH activity of the fusion protein. Effect of OAA on the steady-state rate ( $v_1$ ) of oxidation of malate (10 mM) by NAD (4 mM) in 40 mM phosphate buffer, pH 8.1, catalysed by the fusion protein (92 U·L<sup>-1</sup>).

the absence of OAA and presence of varied concentrations of NADH. This gave  $\beta_2 = 0.0112 (\pm 0.0005) \mu\text{M}^{-1}$ . The parameter  $\beta_3$  was found to be too small (less than  $0.001 \mu\text{M}^{-2}$ ) to have any detectable effect on the reaction kinetics at OAA and NADH concentrations below 50  $\mu\text{M}$ ; it was put equal to zero in all simulations reported below.

The denominator term containing  $q$  in Eqns (1) and (3) reflects the product inhibition contributed by the approach to equilibrium conditions. The equilibrium constant  $K_{\text{eq}}$  for the oxidation of malate by NAD<sup>+</sup> under the present experimental conditions was determined by measurement of the amount of NADH formed after catalytic equilibration of a reaction mixture containing high known concentrations of malate and NAD<sup>+</sup>. This gave  $K_{\text{eq}} = 9.9 \times 10^{-6}$ , corresponding to  $q = 2.5 \times 10^9 \text{ M}^{-2}$  for 10 mM malate and 4 mM NAD<sup>+</sup>.

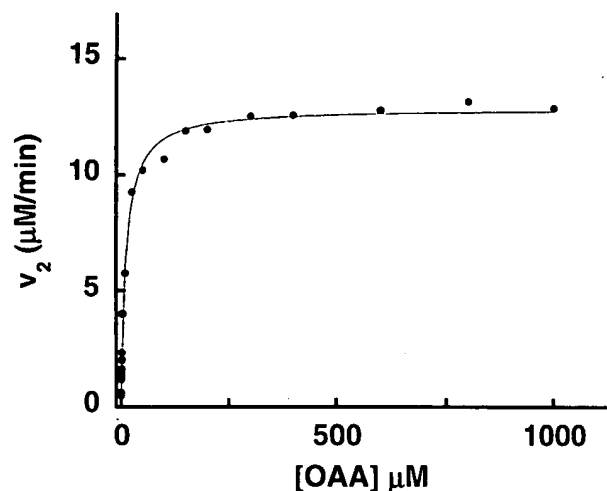


Fig. 3. CS activity of the fusion protein. Steady-state rate ( $v_2$ ) of the reaction of varied concentrations of OAA with acetyl-CoA (0.1 mM) in 40 mM phosphate buffer, pH 8.1, catalysed by the fusion protein (92 U·L<sup>-1</sup>).

### Michaelian parameters for reactions involving OAA

Figure 3 shows initial steady-state velocities ( $v_2$ ) recorded for the CS activity of the fusion protein in the presence of 0.1 mM acetyl-CoA and varied concentrations of OAA. As would be expected from previous reports [17], the Michaelis-Menten equation

$$v_2 = \frac{V[\text{OAA}]}{K_m + [\text{OAA}]} \quad (3)$$

could be well fitted to the experimental data, giving the best-fit estimates  $V = 140 (\pm 8) \text{ nmol} \cdot \text{min}^{-1} \cdot \text{U}^{-1}$  and  $K_m = 11.9 (\pm 0.8) \mu\text{M}$ .

Parameters defined by the steady-state rate equation

$$v_3 = \frac{k'_{\text{cat}}[\text{OAA}]c_e}{K_m + [\text{OAA}]} \quad (4)$$

for the action of AAT (active site concentration  $c_e$ ) on OAA in the presence of 4 mM glutamate were similarly determined. This gave  $k'_{\text{cat}} = 69 (\pm 1) \text{ s}^{-1}$  and  $K'_m = 133 (\pm 6) \mu\text{M}$ .

### Rate behaviour predicted by a free-diffusion mechanism

As substrates in the reactions now considered are present in large excess to the proteins, enzymic species in Fig. 1 can be assumed to be in a steady state over the time-hierarchy where the main changes in concentration of nonenzymic reactants occur. Provided that reactions are carried out for such a short period of time that the high initial concentrations of the substrates malate, NAD<sup>+</sup>, acetyl-CoA, and glutamate remain essentially unchanged, one has to consider only the changes in concentration of the reactants OAA and NADH to account for the time-course of formation of the products citrate and CoA. The time-dependence of the latter four concentration variables can be readily expressed if the transfer of OAA occurs by a free-diffusion mechanism, and is governed by the differential equations

$$\frac{d[\text{NADH}]}{dt} = v_1 \quad (5)$$

$$\frac{d[\text{OAA}]}{dt} = v_1 - v_2 - v_3 \quad (6)$$

$$\frac{d[\text{citrate}]}{dt} = \frac{d[\text{CoA}]}{dt} = v_2 \quad (7)$$

where  $v_3$ ,  $v_1$ , and  $v_2$  denote the steady-state rates of the reactions catalysed by, respectively, AAT and the MDH and CS moieties of the fusion protein.

### Kinetics of the coupled reaction

Figure 4 shows the time-course of CoA formation in the coupled reaction initiated by the addition of catalytic amounts of the fusion protein (92 U·L<sup>-1</sup>) to a 40-mM phosphate buffer solution (pH 8.1) containing fixed high concentrations of the substrates malate (10 mM), NAD<sup>+</sup> (4 mM), and acetyl-CoA (0.1 mM). The time-dependence expected for concentration variables in this reaction (if it proceeds by free diffusion) was calculated by numerical solution of Eqns (5–7) for  $v_3 = 0$  with the assumption that Eqns (1–3) apply, and using the kinetic parameter values reported in the previous sections. The results are given in Fig. 5. The calculated trajectory for the concentration of CoA, multiplied with the absorption coefficient ( $\epsilon = 13\,600 \text{ M}^{-1} \cdot \text{cm}^{-1}$ ) for the chromophore used to

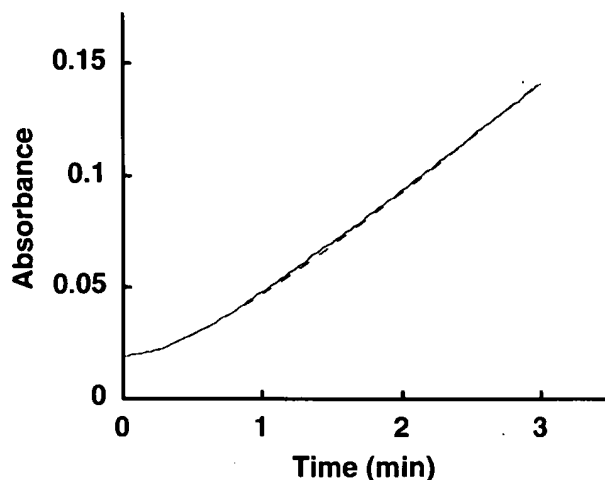


Fig. 4. Time-course of the fusion-protein-catalysed coupled reaction. Absorbance changes recorded at 412 nm for the conversion of malate into citrate and CoA. Conditions as in Fig. 2, except that reactions were performed in the presence of 0.1 mM acetyl-CoA and 0.4 mM dithionitrobenzoate. The dashed curve indicates the absorbance changes expected for a free-diffusion mechanism.

monitor the formation of CoA experimentally, is included in Fig. 4 for comparison with the experimentally recorded trace. It accounts within experimental precision for the observed time-course of CoA formation over the entire reaction time interval examined (0–3 min).

#### Effect of aspartate aminotransferase

Figure 6 shows the inhibitory effect of varied concentrations of aspartate aminotransferase on the pseudo steady-state rate of the coupled reaction catalysed by the fusion protein ( $82 \text{ U}\cdot\text{L}^{-1}$ ) under the conditions of the experiment in Fig. 4. The effect expected for a free-diffusion mechanism was estimated from reaction trajectories calculated by numerical solution of

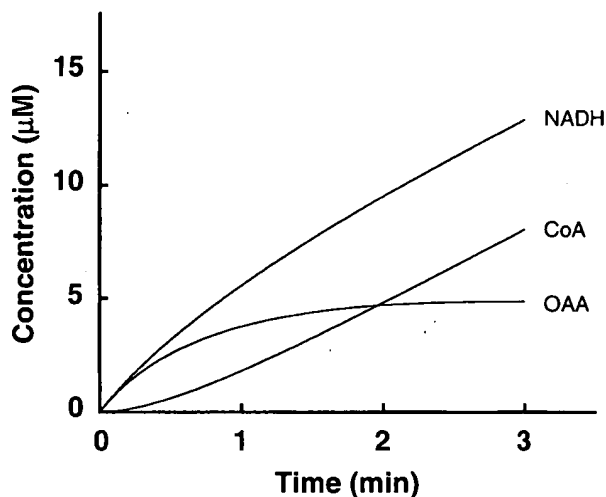


Fig. 5. Calculated time-course of reactant concentration changes in the fusion-protein-catalysed coupled reaction. Trajectories obtained by numerical solution of Eqns (1–7) using parameter values reported in the text.

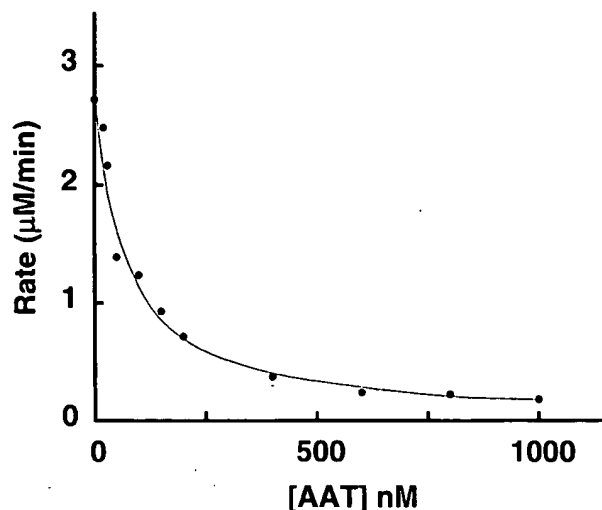


Fig. 6. Effect of AAT on the steady-state rate of the fusion-protein-catalysed coupled reaction. Conditions as in Fig. 4, except that reactions were performed in the presence of varied concentrations of AAT and that the concentration of fusion protein was  $82 \text{ U}\cdot\text{L}^{-1}$ . The curve drawn represents reaction rates expected for a free-diffusion mechanism.

Eqns (5–7) with the assumption that Eqns (1–4) apply and using the kinetic parameter values reported in the previous sections. The results are included in Fig. 6 and show that there is an excellent agreement between the calculated steady-state rates and those observed experimentally over the entire range of AAT concentrations tested (10–1000 nM).

Furthermore, the transient approach of the inhibited reactions towards the pseudo steady-state invariably could be satisfactorily accounted for in terms of a free-diffusion mechanism. This is illustrated in Fig. 7 by example of the results obtained for reactions carried out in the presence of 10, 50, and 600 nM AAT. Inspection of Fig. 7 shows that the transient lag time decreases with increasing concentrations of AAT and eventually

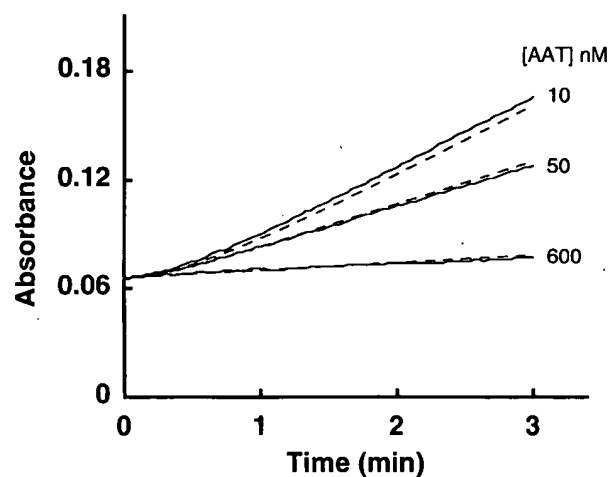


Fig. 7. Effect of AAT on the transient phase of the fusion-protein-catalysed coupled reaction. Time-course of absorbance changes recorded at 412 nm for reactions performed in the presence of 10, 50, and 600 nM AAT under the conditions in Fig. 6. Dashed curves show the absorbance changes expected for a free-diffusion mechanism, as calculated by numerical solution of Eqns (2–8).

becomes immeasurably short. This effect was not detected by Lindbladh *et al.* [11] over the more limited range of AAT concentrations tested by them.

## DISCUSSION

### Consistency of the kinetic data with a free-diffusion mechanism

The fusion protein of malate dehydrogenase and citrate synthase examined in this investigation is identical with that described by Lindbladh *et al.* [11], except that a His-tag was introduced at the N-terminus to facilitate purification of the protein [12]. This His-tag modification has been found not to affect the kinetic properties of the porcine variant of the fusion protein [12] and the kinetic results now obtained with the yeast variant do not differ in any essential respect from those previously reported. The main new information provided here does not concern the actual rate behaviour of the fusion protein, but the mechanistic interpretation of the rate behaviour.

Lindbladh *et al.* [11], in their analysis of the kinetics of the coupled reaction catalysed by the fusion protein, assumed that the expected time-course for a free-diffusion reaction should agree with that observed for an adequately composed mixture of the free enzymes; the differences in kinetic properties of the free enzymes and the corresponding moieties of the fusion protein were considered to be small enough to justify such an approach. In this investigation, we have taken the more direct approach of basing all predictions of the rate behaviour of the fusion protein on the kinetic properties of the fusion protein itself. This means that the expected kinetics of the reaction system in Fig. 1 can be unambiguously established by solution of Eqns (5–7) in case a free-diffusion mechanism applies.

The results in Figs 4 and 5 therefore provide the indisputable inference that the first 3 min of the observed time-course of the fusion-protein-catalysed malate to citrate conversion can be excellently accounted for with the assumption that the reaction conforms to the scheme in Fig. 1 with OAA transfer by free diffusion. This observation has direct bearing on the mechanistic problem now considered; conclusions drawn by Lindbladh *et al.* [11] were based on the behaviour of the fusion protein in the reaction phase reflecting the transient approach to steady-state conditions, and this reaction phase is well covered by the data in Fig. 4.

### Arguments previously presented in support of channelling

Lindbladh *et al.* [11] argued that transient lag times for the coupled reaction catalysed by the fusion protein are indicative of OAA channelling because they are much shorter than expected for a free-diffusion mechanism. The results in Fig. 4 invalidate this argument by showing that the experimental trace during the first 3 min of the reaction differs insignificantly from that calculated for a free-diffusion mechanism. This means that the observed transient time, as well as the observed steady-state rate of the reaction, agrees with that predicted by the kinetic properties of the MDH and CS moieties of the fusion protein. As the transient time and steady-state rate both reflect the steady-state level of OAA that is reached after the transient reaction phase, data in Fig. 4 provide clear evidence that OAA attains a steady-state concentration agreeing with that expected for a free-diffusion mechanism. The data lend no support to the idea that the fusion protein acts upon a catalytically effective concentration of the intermediate OAA that is higher than the

concentration of OAA in bulk solution or otherwise leading to a more rapid transfer of OAA than that obtained by free diffusion.

In view of these results, the observation [11] that the transient time for the coupled reaction is longer with the free enzymes than with the fusion protein loses relevance with regard to the mechanism of action of the fusion protein and merely indicates that a higher steady-state level of OAA is reached with the free enzymes. Such a difference in behaviour of the two systems seems to be fully consistent with the reported differences in  $K_m(\text{OAA})$  values for the MDH and CS activities of the free and fused enzymes [11]. The net balance of these  $K_m$  value differences is in the direction that would be expected to favour a lower steady-state level of OAA in the fusion protein.

Similar considerations apply for the effect of AAT on the fusion-protein-catalysed coupled reaction. Data in Figs 6,7 establish that the experimentally determined effects of AAT on the steady-state and presteady-state time-course of the reaction are in satisfactory agreement with those expected for a free-diffusion mechanism according to the rate parameter estimates obtained for the enzymic activities involved. Consequently, there is no longer any reason to believe that the fusion protein sequesters the intermediate OAA and prevents it from being fully accessible to AAT. The observation that the coupled reaction is more strongly inhibited by AAT when catalysed by the free enzymes is rendered irrelevant by the results in Figs 6,7 and has to be explained in terms of the existing differences in kinetic parameter values for the free and fused enzymes.

### General conclusions

Summing up the above discussion, the present results invalidate the main kinetic arguments that led Lindbladh *et al.* [11] to propose that there is a channelled transfer of the intermediate OAA in the coupled reaction catalysed by the fusion protein. It may now be concluded that the rate behaviour of the fusion protein of yeast MDH and CS is fully consistent with that expected for a free-diffusion mechanism of OAA transfer. This finding provides some additional inferences of general interest.

First, ambiguities obviously arise when the kinetics of coupled reactions catalysed by fusion proteins are interpreted using the rate behaviour of the free enzymes as a predictive model of the expected free-diffusion behaviour of the fused enzymes. All claims so far made for the kinetic detection of metabolite channelling in fusion proteins would seem to have been based on such an interpretational approach. There is reason to consider these claims as tentative until they have been confirmed by less ambiguous methods such as the one described in this investigation.

Second, bringing two sequential enzymes together in a fusion protein (or, by inference, in a bienzyme complex or through adjacent attachment to cell structures) is obviously not sufficient to cause any kinetically significant metabolite channelling through proximity effects. This is consistent with the conclusion drawn by Elcock & McCammon [18] from Brownian dynamics simulation studies of a tentative model structure of the fusion protein of MDH and CS, which indicated that less than 1% of the OAA molecules produced at the MDH site would be directly (i.e. without prior release to solution) transferred to the CS site through Brownian motion alone.

However, Elcock & McCammon [18] also found that a positive electrostatic surface exists between the two enzymic sites, and that the inclusion of electrostatic interactions in the Brownian dynamics simulations increased the estimated direct transfer efficiency to around 45%. This lead them to propose that electrostatic surface diffusion accounts for a highly

efficient channelling of OAA in the fusion protein, and subsequent theoretical work [19] indicated that this proposal could be reconciled with the kinetic effects that Lindbladh *et al.* [11] attributed to channelling. The present results call for a revaluation of the calculations performed by Elcock and collaborators [18,19] and lend no support to their proposal. The data in Figs 4–7 establish that if surface diffusion contributes to the transfer of OAA, then these contributions are too small to bring the MDH-produced OAA out of apparent equilibrium with bulk solution and to cause any kinetically significant deviations from the rate behaviour predicted by a free-diffusion mechanism.

Finally, it should be mentioned that Eqns (5–7) were derived with the tacit assumption that the MDH and CS moieties of the fusion protein operate independently of each other, such that kinetic parameters for the MDH activity remain unaffected by catalytic events at the CS site (and vice versa). The validity of this noncooperativity assumption is corroborated by the agreement between calculated and observed data in Figs 4–7. The only detectable kinetic consequence of the fusion of the two enzymes therefore is the previously reported modification of the kinetic parameter values for the MDH and CS activities from those of the free enzymes to those of the fusion protein [11]. These parameter modifications (and the underlying rate constant changes) could be of biological interest as an illustration of effects that might be caused by complex formation between consecutive enzymes in metabolic pathways. For example, and by analogy to what seems to be the case for the fusion protein of MDH and CS, changes in the kinetic parameter values could result in lower steady-state levels of accumulating intermediates and hence in shorter transient times for the response of the pathway to changes in the environmental conditions. Such parameter-related effects have nothing to do with metabolite channelling, however, but can be adequately described and understood in terms of metabolite transfer by free diffusion.

## ACKNOWLEDGEMENTS

This investigation was supported by grants from The Crafoord Foundation and The Swedish Natural Science Research Council.

## REFERENCES

1. Agius, L. & Sherratt, H.S.A. (1997) Introduction. In *Channelling in Intermediary Metabolism* (Agius, L. & Sherratt, H.S.A., eds), pp. 1–11. Portland Press, London, UK.
2. Cornish-Bowden, A. (1997) Kinetic consequences of channelling. In *Channelling in Intermediary Metabolism* (Agius, L. & Sherratt, H.S.A., eds), pp. 53–70. Portland Press, London, UK.
3. Ovádi, J. (1991) Physiological significance of metabolite channelling. *J. Theor. Biol.* 152, 1–22.
4. Keleti, T., Ovádi, J. & Batke, J. (1989) Kinetic and physico-chemical analysis of enzyme complexes and their possible role in the control of metabolism. *Prog. Biophys. Mol. Biol.* 53, 105–152.
5. Sreere, P.A. (1987) Complexes of sequential metabolic enzymes. *Annu. Rev. Biochem.* 56, 21–56.
6. Welch, G.R. & Easterby, J.S. (1994) Metabolic channelling versus free diffusion: transition-time analysis. *Trends Biochem. Sci.* 19, 193–197.
7. Koch-Schmidt, A.-C., Mattiasson, B. & Mosbach, K. (1977) Aspects on microenvironmental compartmentation. *Eur. J. Biochem.* 81, 71–78.
8. Bülow, L. (1987) Characterization of an artificial bifunctional enzyme  $\beta$ -galactosidase-galactokinase prepared by gene fusion. *Eur. J. Biochem.* 163, 443–448.
9. Ljungcrantz, P., Carlsson, H., Mansson, M.O., Buckel, P., Mosbach, K. & Bülow, L. (1989) Construction of an artificial bifunctional enzyme  $\beta$ -galactosidase-galactose dehydrogenase exhibiting efficient galactose channelling. *Biochemistry* 28, 8786–8792.
10. Bülow, L. & Mosbach, K. (1991) Multienzyme systems obtained by gene fusion. *Trends Biotechnol.* 9, 226–231.
11. Lindbladh, C., Rault, M., Hagglund, C., Small, W.C., Mosbach, K., Bülow, L., Evans, C. & Sreere, P.A. (1994) Preparation and kinetic characterization of a fusion protein of yeast mitochondrial citrate synthase and malate dehydrogenase. *Biochemistry* 33, 11692–11698.
12. Shatalin, K., Lebreton, S., Rault-Leonard, M., Vélot, C. & Sreere, P.A. (1999) Electrostatic channelling of oxaloacetate in a fusion protein of porcine citrate synthase and porcine mitochondrial malate dehydrogenase. *Biochemistry* 38, 881–889.
13. Harada, K. & Wolfe, R.G. (1968) Malic dehydrogenase: a kinetic study of hydroxymalonate inhibition. *J. Biol. Chem.* 243, 4123–4130.
14. Polyakovskiy, O.L., Demidkina, T.V. & Egorov, C.A. (1972) The position of an essential tyrosine residue in the poly peptide chain of aspartate transaminase EC-1.6.1.1. *FEBS Lett.* 23, 262–264.
15. Bradford, M.M. (1976) A rapid and sensitive method for the quantitation of microgram quantities of protein using the principle of protein-dye binding. *Anal. Biochem.* 72, 248–254.
16. Heyde, E. & Ainsworth, S. (1968) Kinetic studies on the mechanism of the malate dehydrogenase reaction. *J. Biol. Chem.* 243, 2413–2423.
17. Johansson, C.-J. & Pettersson, G. (1974) Evidence that citrate synthase operates by an ordered ternary-complex mechanism. *Eur. J. Biochem.* 42, 383–388.
18. Elcock, A.H. & McCammon, J.A. (1996) Evidence for electrostatic channelling in a fusion protein of malate dehydrogenase and citrate synthase. *Biochemistry* 35, 12652–12658.
19. Elcock, A.H., Huber, G.A. & McCammon, J.A. (1997) Electrostatic channelling of substrates between enzyme active sites. Comparison of simulation and experiment. *Biochemistry* 36, 16049–16058.

## Exhibit F

**Table 1:** Values that allow calculation of the ratios of sialyltransferase activities using either the corrected specific activities or the turnover numbers. The ratio is **2.22** using either the corrected specific activities or the turnover numbers.

Enzyme	Mass (Da)	Sialyltransferase content (%)	Specific activity (U/mg)	Corrected specific activity (U/mg)	Turnover number (sec <sup>-1</sup> )
Fusion FUS-01/2	70,398	61.5	2.73	4.44	3.20
Sialyltransferase	43,304	100	2.00	2.00	1.44

**Table 2:** Values that allow calculation of the ratios of CMP-NeuAc synthetase activities using either the corrected specific activities or the turnover numbers. The ratio is **1.27** using either the corrected specific activities or the turnover numbers.

Enzyme	Mass (Da)	CMP-NeuAc synthetase content (%)	Specific activity (U/mg)	Corrected specific activity (U/mg)	Turnover number (sec <sup>-1</sup> )
Fusion FUS-01/2	70,398	38.5	33.66	87.43	39.5
CMP-NeuAc synth.	27,313	100	69.00	69.00	31.4

**Note:** both individual enzymes have C-terminal tags, so their added mass is slightly larger (by 0.45%) than the fusion enzyme.

## **EXHIBIT F**

**This Page is Inserted by IFW Indexing and Scanning  
Operations and is not part of the Official Record**

**BEST AVAILABLE IMAGES**

Defective images within this document are accurate representations of the original documents submitted by the applicant.

Defects in the images include but are not limited to the items checked:

- ☐ BLACK BORDERS
- ☐ IMAGE CUT OFF AT TOP, BOTTOM OR SIDES
- ☒ FADED TEXT OR DRAWING
- ☒ BLURRED OR ILLEGIBLE TEXT OR DRAWING
- ☐ SKEWED/SLANTED IMAGES
- ☐ COLOR OR BLACK AND WHITE PHOTOGRAPHS
- ☐ GRAY SCALE DOCUMENTS
- ☒ LINES OR MARKS ON ORIGINAL DOCUMENT
- ☐ REFERENCE(S) OR EXHIBIT(S) SUBMITTED ARE POOR QUALITY
- ☐ OTHER: \_\_\_\_\_

**IMAGES ARE BEST AVAILABLE COPY.**

**As rescanning these documents will not correct the image problems checked, please do not report these problems to the IFW Image Problem Mailbox.**